การเตรียมเส้นใยระดับนาโนเมตรอิเล็กโทรสปันซิลิกาที่มีโครงสร้างมีโซพอรัสแบบควบคุมผ่านการจัดเรียงตัวเองของสารลดแรงตึงผิว

นางสาวอรรจน์ชญาน์ สุวรรณสุนทร

วิทยานิพนธ์นี้เป็นส่วนหนึ่งของการศึกษาตามหลักสูตรปริญญาวิทยาศาสตรมหาบัณฑิต
สาขาวิชาเคมี ภาควิชาเคมี
คณะวิทยาศาสตร์ จุฬาลงกรณ์มหาวิทยาลัย
ปีการศึกษา 2559

PREPARATION OF ELECTROSPUN SILICA NANOFIBERS WITH CONTROLLED MESOPOROUS STRUCTURE VIA SURFACTANT SELF-ASSEMBLY

Miss Athchaya Suwansoontorn

A Thesis Submitted in Partial Fulfillment of the Requirements
for the Degree of Master of Science Program in Chemistry
Department of Chemistry
Faculty of Science
Chulalongkorn University
Academic Year 2016

Thesis Title	PREPARATION OF ELECTROSPUN SILICA NANOFIBERS WITH CONTROLLED MESOPOROUS STRUCTURE VIA SURFACTANT SELF-ASSEMBLY
By	Miss Athchaya Suwansoontorn
Field of Study	Chemistry
Thesis Advisor	Assistant Professor Puttaruksa Varanusupakul, Ph.D.

Accepted by the Faculty of Science, Chulalongkorn University in Partial Fulfillment of the Requirements for the Master's Degree

.....Dean of the Faculty of Science
(Associate Professor Polkit Sangvanich, Ph.D.)

THESIS COMMITTEE

.....Chairman
(Associate Professor Vudhichai Parasuk, Ph.D.)

.....Thesis Advisor
(Assistant Professor Puttaruksa Varanusupakul, Ph.D.)

.....Examiner
(Associate Professor Thumnoon Nhujak, Ph.D.)

.....External Examiner
(Apinya Navakhun, D.Sc.)

อรรจน์ชญาน์ สุวรรณสุนทร : การเตรียมเส้นใยระดับนาโนเมตรอิเล็กโทรสปันซิลิกาที่มีโครงสร้างมีโซพอรัสแบบควบคุมผ่านการจัดเรียงตัวเองของสารลดแรงตึงผิว (PREPARATION OF ELECTROSPUN SILICA NANOFIBERS WITH CONTROLLED MESOPOROUS STRUCTURE VIA SURFACTANT SELF-ASSEMBLY) อ.ที่ปรึกษาวิทยานิพนธ์หลัก: ผศ. ดร.พุทธรักษา วรานุศุภากุล, 66 หน้า.

เส้นใยระดับนาโนเมตรอิเล็กโทรสปันซิลิกาเป็นวัสดุที่ได้รับความสนใจในการทำตัวตรวจวัดหรือ วัสดุดูดซับ แม้ว่าเส้นใยระดับนาโนเมตรอิเล็กโทรสปันมีพื้นที่ผิวสูง แต่นักวิจัยยังคงพัฒนาประสิทธิภาพของเส้นใยโดยการสร้างโครงสร้างรูพรุนภายในเส้นใย วิธีหนึ่งที่ใช้คือการใช้ไมเซลล์ของสารลดแรงตึงผิวเป็นแม่แบบของโครงสร้างรูพรุน อย่างไรก็ตามผลของไมเซลล์ของสารลดแรงตึงผิวที่มีต่อโครงสร้างรูพรุนในเส้นใยยังคงเป็นหัวข้อที่ศึกษากันอยู่ ดังนั้น ในงานวิจัยนี้จึงศึกษาผลกระทบของสารลดแรงตึงผิวที่มีต่อโครงสร้างรูพรุนภายในเส้นใยระดับนาโนเมตรอิเล็กโทรสปันซิลิกา โดยทำการศึกษาสารลดแรงตึงผิวสองประเภท สารลดแรงตึงผิวที่มีประจุบวกและสารลดแรงตึงผิวที่ไม่มีประจุ สารลดแรงตึงผิวที่มีประจุบวกที่มีสายโซ่แอลคิลต่างกัน ได้แก่ เฮกซะเดซิลไตรเมทิลแอมโมเนียมโบร์ไมด์ (CTAB) ได-เอ็น-แอลคิล-ไดเมทิล-แอมโมเนียม คลอไรด์ (DAAC) และ เอ็น-ออกทิลไตรเมทิลแอมโมเนียมโบร์ไมด์ (OTAB) และสารลดแรงตึงผิวที่ไม่มีประจุ ได้แก่ พลูโรนิค F127 ตรวจสอบลักษณะทางกายภาพของเส้นใยด้วยเทคนิค FTIR, SEM, TEM และการดูดซับของไนโตรเจน เส้นใยที่เตรียมได้มีโครงสร้างรูพรุนภายในเส้นใย โดยความเข้มข้นของสารลดแรงตึงผิวบางชนิดส่งผลต่อลักษณะของเส้นใย นอกจากนี้กระบวนการ โซล-เจล ถูกชะลอเมื่อใช้สารลดแรงตึงผิวที่มีหมู่แอลคิลสายสั้นความเข้มข้นสูง โดยไปขัดขวางการสร้างโครงสร้างซิลิกา นอกจากนี้ชนิดและความเข้มข้นของสารลดแรงตึงยังส่งผลต่อพื้นที่ผิว รูปร่างของรูพรุนและความสม่ำเสมอของโครงสร้างรูพรุน สุดท้ายนำเส้นใยซิลิกาที่เตรียมได้ไปใช้ในการกำจัดสีย้อม เส้นใยระดับนาโนเมตรอิเล็กโทรสปันซิลิกามีประสิทธิภาพในการกำจัดสีย้อมดีกว่าซิลิกาเจลทางการค้า

ภาควิชา เคมี ลายมือชื่อนิสิต .....

สาขาวิชา เคมี ลายมือชื่อ อ.ที่ปรึกษาหลัก .....

ปีการศึกษา 2559

5772210323 : MAJOR CHEMISTRY

KEYWORDS: ELECTROSPUN / SILICA NANOFIBERS / SURFACTANT / SELF-ASSEMBLY

ATHCHAYA SUWANSOONTORN: PREPARATION OF ELECTROSPUN SILICA NANOFIBERS WITH CONTROLLED MESOPOROUS STRUCTURE VIA SURFACTANT SELF-ASSEMBLY. ADVISOR: ASST. PROF. PUTTARUKSA VARANUSUPAKUL, Ph.D., 66 pp.

Silica electrospun nanofibers has been an interesting material for sensors or sorbents. Even though the electrospun nanofibers have high specific surface area, the researchers still improve their performance by creating porous structure in nanofibers. One of the methods is the use of surfactant micelle as a template for porous structure in nanofibers. However, the effect of surfactant micelle on porous structure in nanofibers is still a topic of discussion. Therefore, in this study various surfactants were examined for the effect on porous structure in electrospun silica nanofibers. Two types of surfactant were examined; cationic surfactant and non-ionic surfactant. Cationic surfactant with different non-ionic chain which are hexadecyl-trimethyl-ammonium bromide (CTAB), di-n-alkyl-dimethyl-ammonium chloride (DAAC), and n-octyl-trimethyl-ammonium bromide (OTAB) and non-ionic surfactant which is Pluronic F127 (PF) were studied. The characteristics of nanofibers were examined by FTIR, SEM, TEM, nitrogen physisorption and image analysis. The nanofibers with porous structure were observed. The concentration of some surfactants slightly impacted the morphology of nanofibers. In addition, the sol-gel process was interrupted when short alkyl chain surfactant was used at high concentration which prevents the formation of silica network structure. Moreover, the types and concentrations of surfactant affected the surface area, pore shape and uniformity of porous structure in silica nanofibers. Finally, the fabricated silica nanofibers were applied for a dye removal. The silica electrospun nanofibers showed a better efficiency in dye removal than the commercial silica gel.

Department:	Chemistry	Student's Signature	.....
Field of Study:	Chemistry	Advisor's Signature	.....
Academic Year:	2016		

ACKNOWLEDGEMENTS

The author would like to offer my special thanks to many people for their helpful in this research. This research can be successfully completed with support from Assistant Professor Dr. Puttaruksa Varanusupakul, my research advisor, who has been giving useful guidance and commentary. Besides my advisor, I would like to thank the rest of my thesis committees: Associate Professor Dr. Vudhichai Parasuk, Associate Professor Dr. Thumnoon Nhujak, and Dr. Apinya Navakhun for their insightful and valuable suggestion.

Moreover, I would like to thank my research group for their kind advices and encouragements to finished my research. Without them, my time during Master's degree will be difficult and lifeless.

At last, I also would like to express my sincere gratitude to my family; my parents and my close friends for their love, care and supports.

CONTENTS

Page

Page

Page

LIST OF TABLES

LIST OF FIGURES

LIST OF ABBREVIATIONS AND SYMBOLS

ATR-FTIR	Attenuated total reflectance Fourier-transform infrared spectroscopy
CMC	Critical micelle concentration
CTAB	Hexadecyl-trimethyl-ammonium bromide
DAAC	Di-n-alkyl-dimethyl-ammonium chloride
MB	Methylene blue
OTAB	n-Octyltrimethylammonium bromide
PF	Pluronic F127
PSNs	Polystyrene nanoparticles
PVA	Poly(vinyl alcohol)
SEM	Scanning electron microscope
TEM	Transmission electron microscope
TEOS	Tetraethyl orthosilicate

CHAPTER I
INTRODUCTION

1.1 Statement of purpose

The used of silica nanostructure as sorbents [1, 2], catalysts [3, 4], drug carriers [5] or energy storages [6] was interested nowadays because silica can resist of organic solvent, acid-base solution and high temperature. There are many type of silica nanostructure such as tubes, particles, and fibers. In this research, fibers are interest because of its high surface area per volume which increases the efficiency when used as sorbents or detectors.

The electrospinning is an interesting technique for nanofibers fabrication because of its simplicity. The non-woven nanofibers with high surface area per volume were produced via this technique. Most of the spinning solutions are polymer solution, but polymer is not appropriate when used with organic solution. Therefore, in 2010, Guo et al. [7] fabricated flexible and high-heat resistant silica nanofibers. The silica nanofiber mats were obtained using electrospinning technique with blended solutions between poly(vinyl alcohol) (PVA) and silica gel, then calcined to eliminate the organic compound. The nanofibers morphologies shown that the increasing of polymer can improve nanofibers flexibility. Moreover, the beads in nanofibers were decrease due to the increasing of viscosity in the electrospun solutions.

Even though silica electrospun nanofibers have high surface area, its performance can be improved by producing porous structure in nanofibers. Porous in nanofibers can be formed by using template such as surfactant micelle and nanoparticle. The used of surfactants micelle is one of the well-known methods which use to form porous structure in inorganic materials [8]. For example, Hou et al. [5] were prepared porous silica nanofibers as a drug delivery host carrier via electrospinning process. The porous structure in nanofibers were created using P123 surfactant. The surfactant will form micelle in two different shape, sphere and cylinder, and act as porous template. When surfactant and polymer were removed, silica nanofibers were obtained with porous structure as shown in Figure 1.1.

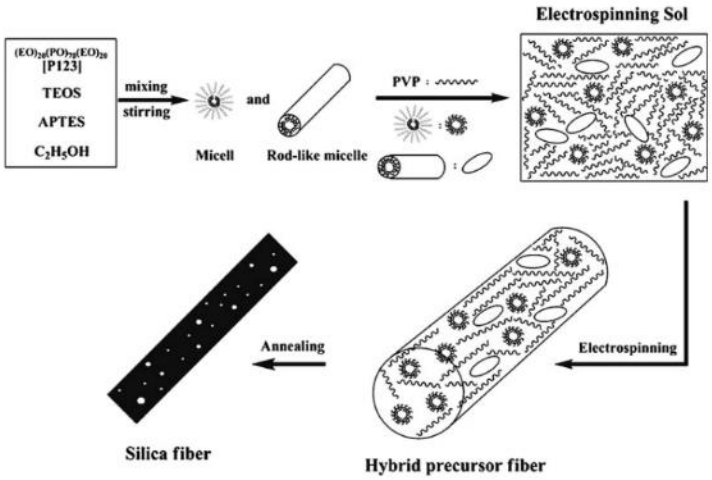

Figure 1.1 The possible formation process of the porous structures in silica fibers [5].

Moreover, the porous in silica using surfactant micelle can be produced via phase separation. In 2013, He et al. [9] prepared silica nanofibers with mesoporous structure via electrospinning and sol-gel method. In this work, Pluronic F127 was used. The results shown that when the solvent evaporates rapidly, surfactant molecules were diffuse along the nanofibers length because surfactant can dissolve in solvent better than in silica-gel. As a result, the mesoporous were formed when surfactant was eliminated. Similarly to Zhou et al. [10] and Nagamine et al. [11] works which use the evaporation of solvent to induce surfactant micelle in the formation of porous structure in silica nanofibers.

Furthermore, the nanoparticles were also used as porous template. As in Wu et al. [1] works, they fabricated porous silica nanofibers by electrospinning technique and used polystyrene nanoparticles (PSNs) as a template for porous structure. The pore size of the silica nanofibers ranges from micropores to mesopores. Moreover, pore size can be controlled by changing the weight ratio of PSNs. The increasing of PSNs concentration leads to the increase of mesopores and surface area.

Silica nanofibers can be applied into various applications. For example, in 2015, Islam et al. [12] prepared phosphine-functionalized PVA/SiO_2 composite nanofibers. The nanofibers were used as adsorbent to remove manganese (Mn^{2+}) and nickle (Ni^{2+})

ions from aqueous solution. Hexadecyl-trimethyl-ammonium bromide (CTAB) were used as porous template and then were eliminated. The nanofibers have more surface area and the removal efficiency of metal ions were improved. And in 2015, Zong et al. [6] prepared electrospun silica nanofibers for adsorption of fatty acid eutectics. The nanofibers were used as storage and retrieval of thermal energy. With its high surface area, the nanofibers have high absorption capacity of fatty acid and have high efficiency of thermal energy storage.

Normally, surfactants are amphiphilic compound which have both hydrophobic and hydrophilic part. With their structure, surfactants can form micelle. In 2015, Zhao et al. [13] studied the self-assembly of long tail surfactant in ethanol. The researcher found that micelle turn into secondary aggregation when water was added as shown in Figure 1.2. The secondary aggregation can be avoided when additive, such as benzenesulfonate counterion or 1-octanol, was added.

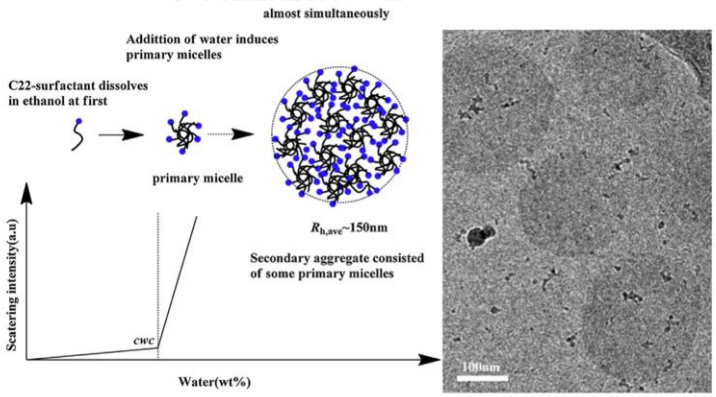

Figure 1.2 Schematic of the aggregation mechanism and cryo-EM micrograph of secondary aggregates [13].

However, the effect of various surfactant micelle on porous structure in nanofibers is still studying. Therefore, in this work, the effect of surfactants on porous structure in electrospun silica nanofibers were investigated. Four different types of surfactant, i.e., CTAB with long single alkyl chain cationic surfactant, DAAC with long double alkyl chain cationic surfactant, OTAB with short single alkyl chain cationic surfactant, and PF with long double alkyl chain non-ionic surfactant were studied at

various concentration. Moreover, the adsorption of dye was examined with the fabricated nanofibers as a sorbent.

1.2 Objective of this research

To studied the effect of surfactant self-assembly on porous structure in electrospun silica nanofibers, and applied the silica nanofibers as a sorbent in dye adsorption.

1.3 Scopes of this research

1.3.1 Preparation of electrospun silica nanofibers with porous structure via surfactant self-assembly.

1.3.2 Characterization of electrospun silica nanofibers by SEM, TEM, ATR-FTIR, and nitrogen physisorption measurement.

1.3.3 The effect of surfactant self-assembly on porous structure in electrospun silica nanofibers.

1.3.4 The adsorption of dye using electrospun silica nanofibers.

1.4 Benefits of this research

The research aimed to understand the effect of surfactant to porous structure in electrospun silica nanofibers and used as sorbents for adsorption of dye in water.

CHAPTER II

THEORY

2.1 Silica

Silicon dioxide (SiO_2), known as silica, is a white, colorless, chemical compound which are made of silicon (Si) and oxygen (O). Silica is the main compound of more than 95 percent of rocks and 59 percent of Earth's crust. Silica is water and organic solvent insoluble, and has a high melting point. Silica has been used in various industrial applications including some food and beverage industry. [14]

Silica has a huge structure with each silicon atom bounded with four oxygen atoms, and each oxygen atom to two silicon atoms as shown in Figure 2.1. At the surface of silica, the structure terminates with siloxane links, Si-O-Si, or silanol groups, Si-OH. Silianol group is happened from the incomplete of condensation during polymerization process. Silanol groups on the surface can adsorb the polarised molecules and electron donor molecules by hydrogen bonds. In addition, the deprotonation of silanol on the surface can be occurs in basic solutions, then cation adsorption can take place. [15, 16]

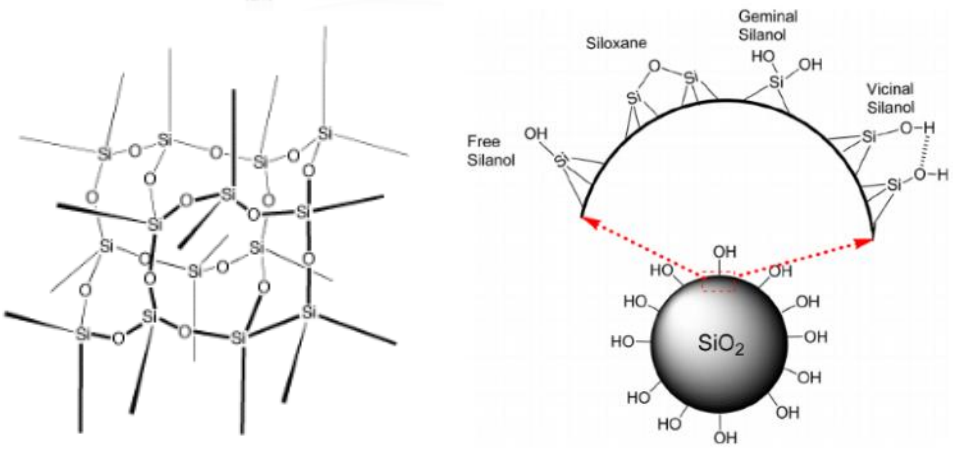

a) b)

Figure 2.1 Schematic of a) silica structure [17] and b) silanol group at the surface [18].

2.2 Preparation of silica via sol-gel process

Sol-gel process is a chemical synthesis technique for preparing gels, glasses, and ceramic powders. This method is used for the fabrication of metal oxides, for example the oxides of silica which undergo hydrolysis and condensation polymerization reactions to give gels.

Silica gels can be prepared from sol-gel polymerization of silicon alkoxides, such as tetraethyl orthosilicate (TEOS). The first step is hydrolysis of TEOS in solvent, generally ethanol. The silanols (Si-OH) were produced, but the complete hydrolysis of TEOS to silicic acid or $Si(OH)_4$ would not occur. Instead of complete hydrolysis of TEOS, the condensation may occur between two silanols or a silanol and an ethoxy group to form a siloxane group (Si-O-Si). However, both hydrolysis and condensation may need acid or base catalyst to perform nucleophilic substitution reactions. Under acid conditions, the rapid deprotonation of -OR or -OH substituents bonded to Si will occur, while under basic conditions hydroxyl or silanoate anions directly attack Si. The mechanisms of sol-gel reaction are shown in Figure 2.2 and 2.3.

Acid-Catalyzed Hydrolysis

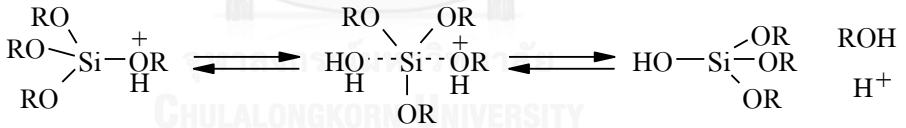

Acid-Catalyzed Condensation

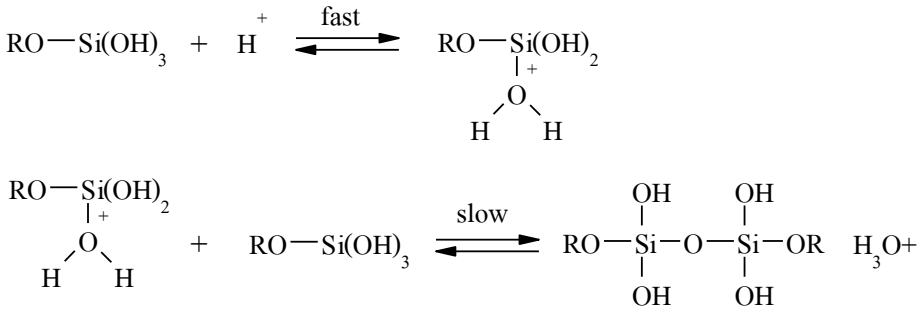

Figure 2.2 Schematic of sol-gel polymerization mechanism of silica with acid catalyst.

Base-Catalyzed Hydrolysis

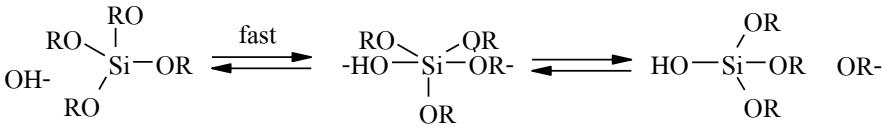

Base-Catalyzed Condensation

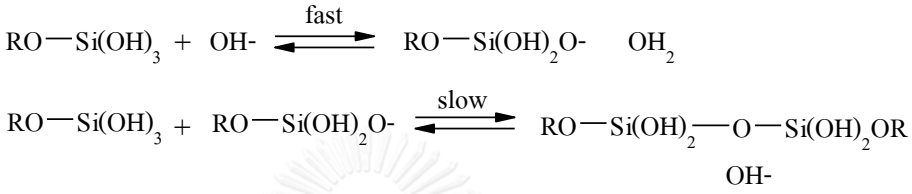

Figure 2.3 Schematic of sol-gel polymerization mechanism of silica with basic catalyst.

At acidic conditions, silica form linear molecules that are sometimes cross-linked as shown in Figure 2.4 a. At basic conditions, silica forms branched cluster molecules as shown in Figure 2.4 b.

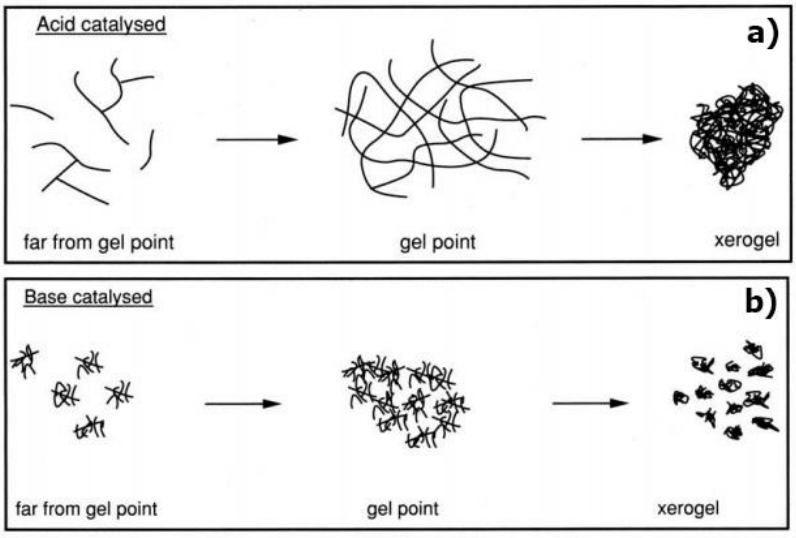

Figure 2.4 Effect of a) acid- and, b) base-catalyst in hydrolysis [19].

When the Si-O-Si bond are formed sufficiently, they become colloidal particles or a sol. The colloidal particles and condensed silica species link to form a 3-dimensional network and the viscosity increases sharply at gelation. The product is called an alcogel. If the solvent is removed by common drying, such as evaporation, the product is called xerogels. If it is removed by supercritical drying, the product is called aerogels as shown in Figure 2.5.

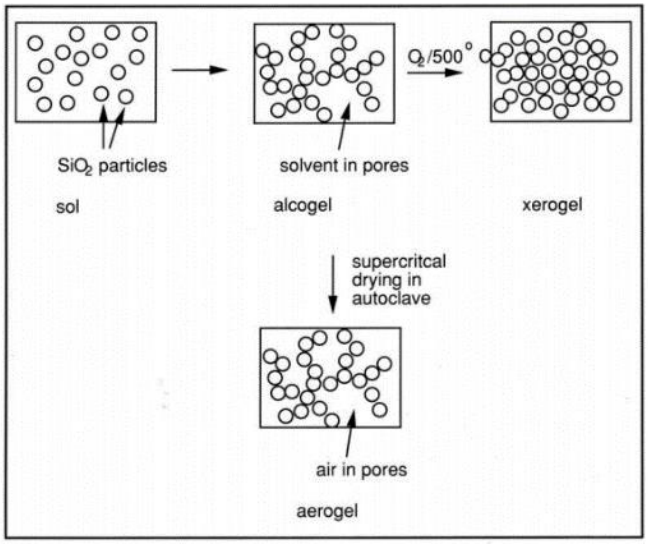

Figure 2.5 Effect of solvent removal [19].

2.3 Surfactant

Surfactant or surface-active agent is a compound that can lower surface tension between two liquids or between liquid and solid. Surfactant may act as detergents, wetting agents, emulsifiers, foaming agents, and dispersants.

Surfactants are usually organic compounds that are amphiphilic. Amphiphilic compound means that the compound contains both hydrophilic and hydrophobic groups. Therefore, surfactant molecule contains both a water soluble and water insoluble component. One of the properties of surfactants is its self-association into organized molecular structures such as micelles, vesicles, microemulsions, bilayers membranes, and liquid crystals [20]. In bulk aqueous phase, surfactants form aggregates, micelles, which hydrophobic part are at the core and hydrophilic part are

contact with aqueous environment. The shape of micelles depends on chemical structure of surfactants. There are many shape of micelles such as sphere, ellipsoid, cylinder or inverted micelle when surfactants are in non-polar phase.

2.3.1 Critical micelle concentration

In colloidal and surface chemistry, the critical micelle concentration (CMC) is the concentration above which micelles form. At low concentration of surfactant, surfactant molecules arrange on the surface. When more concentration is added, surface tension of the solution decreases since more surfactant molecules will be on the surface. When the surface becomes saturated, the excess surfactant molecules will form the micelles as shown in Figure 2.6. This concentration point is called CMC. Moreover, CMC can also be measured when surfactant solution shows dramatically changes in other physical properties such as electrical conductivity, osmotic pressure, density, light scattering, or refractive index.

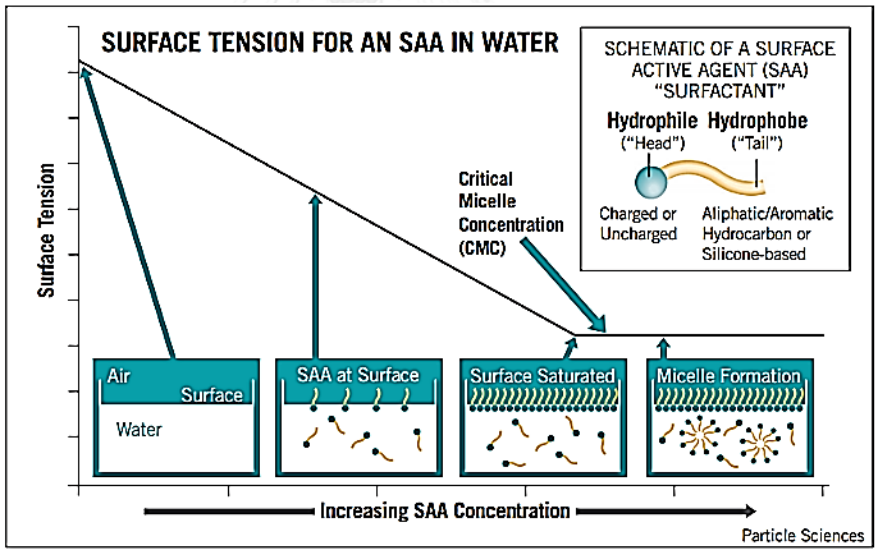

Figure 2.6 Surface tension of a surfactant solution with increasing concentration and formation of surfactant micelles [21].

2.3.2 Types of surfactant

Based on their functional group, there are many types of surfactant as cationic, anionic, zwitterionic, and non-ionic surfactants. [20]

2.3.2.1 Hexadecyl-trimethyl-ammonium bromide (CTAB)

Hexadecyl-trimethyl-ammonium bromide (CTAB) is a quaternary ammonium surfactant with single non-ionic chain. Its cation is an effective antiseptic agent against bacteria and fungi. Mostly used in the extraction of DNA, synthesis of gold nanoparticles and mesoporous silica nanoparticles, and household products such as shampoos and cosmetics. The chemical structure of CTAB is shown in Figure 2.7.

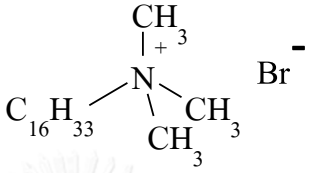

Figure 2.7 Chemical structure of CTAB.

2.3.2.2 Di-n-alkyl-dimethyl-ammonium chloride (DAAC)

Di-n-alkyl-dimethyl-ammonium chloride is a quaternary ammonium, cationic surfactant with double non-ionic chain. The chemical structure of DAAC is shown in Figure 2.8.

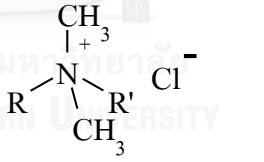

$$R, R' = \text{n-}C_{16}H_{33}\text{ , n-}C_{18}H_{37}$$

Figure 2.8 Chemical structure of DAAC.

2.3.2.3 n-Octyltrimethylammonium bromide (OTAB)

n-Octyltrimethylammonium bromide is a quaternary ammonium, cationic surfactant with single non-ionic chain which is shorter than CTAB's. The chemical structure of OTAB is shown in Figure 2.9.

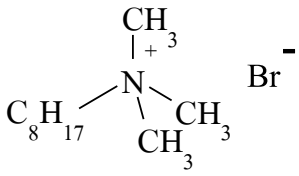

Figure 2.9 Chemical structure of OTAB.

2.3.2.4 Pluronic F127 (PF)

Pluronic F127 or Poloxamers 407 is a non-ionic surfactant. Pluronic F127 is triblock copolymer which consists of two hydrophilic blocks of polyethylene glycol and a central hydrophobic block of polypropylene glycol between two hydrophilic blocks. It is used in some cosmetic, mouthwashes, or contact lens cleaning solutions. The chemical structure of PF is shown in Figure 2.10.

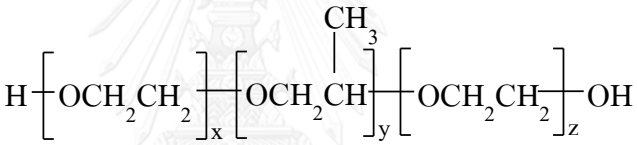

Figure 2.10 Chemical structure of PF.

2.4 Electrospinning

2.4.1 Electrospinning process

Electrospinning is a technique that uses to create fibers by using high electrostatic force. The setup consists of a high voltage power supply, a container of spinning solution with metal needle, and a collector which conductive. The electrospinning setup is shown in Figure 2.11.

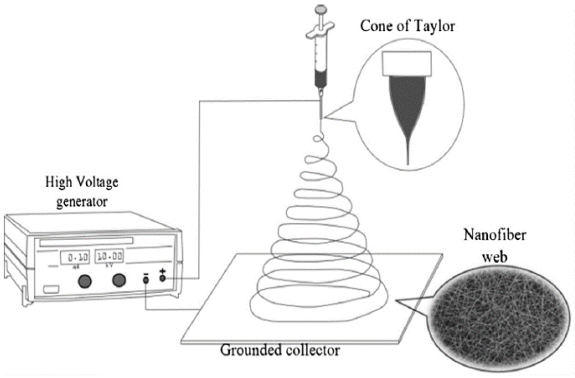

Figure 2.11 Schematic of electrospinning setup with metal sheet collector [22].

When high voltage was applied, the spherical droplet solution at needle tip will change to conical shape called "Taylor's cone". The Taylor's cone formation is shown in Figure 2.12. When the voltage reaches a critical value, the solution will form a continuous nanofiber due to electrostatic force and will be ejected, while the solvent will volatile before nanofibers fall on collector.

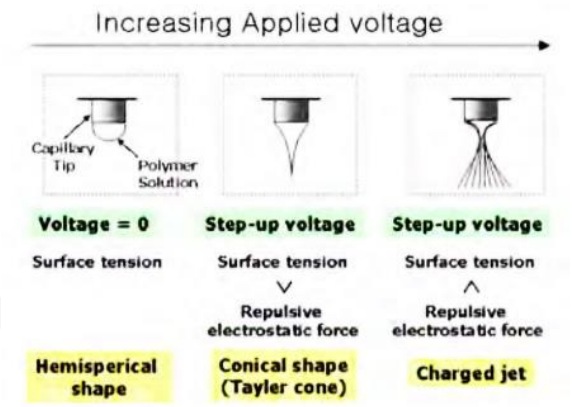

Figure 2.12 Formation of Taylor's cone [23].

Therefore, the nanofibers without solvent and with diameters ranging from nanometers to micrometers were produced. The obtained nanofibers matt has high surface area per volume, then it is appropriate to use as adsorbent materials.

2.4.2 Parameters of electrospinning

There are two groups of parameters which affect the morphology and diameters of electrospun fibers: solution parameters and processing parameters [24].

2.4.2.1 Solution parameters

2.4.2.1.1 Viscosity

Solution viscosity is an important factor in determining the fibers morphology. The very low viscosity leads to non-continuous and rough fibers, whereas very high viscosity results in the hard ejection of jets from solution. The solution viscosity can be controlled by adjusting the polymer concentration of the solution. An increase in concentration, the viscosity and fibers diameter will increase. Molecular weight is also affect fibers morphology. At the same concentration, the polymer with lower molecular weight trends to form beads instead of smooth fibers. Therefore, viscosity, polymer concentration, and polymeric molecular weight are related to each other.

2.4.2.1.2 Surface tension

Surface tension is one of important factors in electrospinning. The high surface tension of electrospinning solution prevents the electrospinning process, the jet will unstable and produce spray of droplets. Reducing the surface tension can prevents beads formation in nanofibers. Surface tension can be adjusted by changing polymer concentration.

2.4.2.1.3 Dielectric constant

The dielectric constant can show how easy that a material can be polarized by electric field. The solution dielectric constant is mainly determined by the polymer type, solvent sort, and salt. The electrical conductivity can be adjusted by adding ionic salts or organic acids. Moreover, dielectric constant affects morphology and diameter of electrospun fibers. An increase of dielectric constant in solution leads to thinner nanofibers.

2.4.2.2 Processing parameters

2.4.2.2.1 Applied electric potential

Applied voltage is an important factor because the charge jet will be ejected from Taylor’s cone and create the electrospun fibers only

when the applied voltage is higher than the threshold voltage. However, the affection of the applied electric potential on the diameter of electrospun fibers is still unclear. Some presented that there just slightly affected on diameter of fibers [25], while some groups suggested that higher voltages facilitated the formation of narrow diameter fiber [26]. In addition, some groups showed that higher voltage offered more beads formation [27, 28].

2.4.2.2.2 Distance from tip to collector

The distance between tip of syringe and collector is also affect the electrospun fibers diameter and morphologies. The distance from tip to collector has an influence on the time spent in the evaporation of solvent and strength of electric field [29]. If the distance is too short, the solvent evaporation time decrease and fibers may not solidify before reaching collector. Meanwhile if the distance is too long, bead fiber can be obtained. Therefore, the optimum distance from tip to collector is recommended for electrospun fiber which is dryness from solvent.

2.4.2.2.3 Flow rate

The difference of flow rate can affect the velocity of the jet fluid, solvent evaporation, and morphology of obtained fibers. Generally, slow flow rate is more recommended as spinning solution will get enough time for solvent evaporation, and smooth fibers will be obtained as a result. If the flow rate is too high, bead and thick fibers will form due to the short drying time.

2.5 Adsorption

Sorption is a physical and chemical process that one substance becomes attached to another. The process can occur at the contact surface between two phases such as liquid - liquid, liquid - solid, liquid - gas, gas - solid.

There are several cases of sorption, for example adsorption and absorption. Adsorption is different from absorption. As shown in Figure 2.13, adsorption means onto two-dimensional surface of the substance, while absorption means into three-dimensional of the substance throughout the bulk.

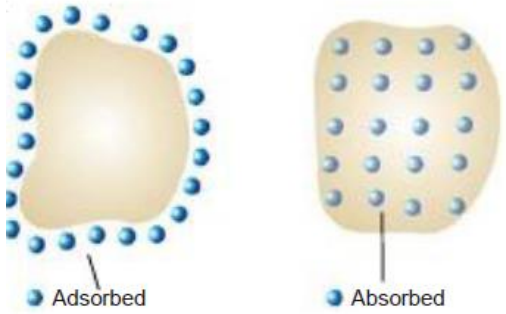

Figure 2.13 Schematic of (a) adsorptive and (b) absorptive process [30].

Adsorption process involves two components, adsorbent and adsorbate. Adsorbent is the substance that adsorption occurs on its surface. Adsorbate is the substance which is adsorbed on the adsorbent surface.

Surface structure, porosity and surface area, is important characteristic compared to chemical composition for adsorption. There are three steps occurs during the adsorption process; (I) film diffusion, when the adsorbate film on the surface of adsorbent, (II) pore diffusion, when the adsorbate through the pores of solid phase, and (III) adsorptive reaction, when the adsorbate interacts with the surface of adsorbent. But adsorbent have limited capacity, the adsorbate may compete for active sites.

The adsorbate can interact with a sorbent in several ways. Adsorbate may interact two dimensional with surface of adsorbent by intermolecular forces, or interact with

electrostatic attraction between charge sites on surface of adsorbent and ionizable adsorbate, or interact with chemical reactive such as covalent bond.

Most of the surface of adsorbents contains nanopores. Then nanopores of adsorbent can divided into three types as shown in Figure 2.14. First, micropores which have diameters smaller than 2 nm. Second, mesopores with diameters are between 2–50 nm. Last, macropores with diameters are larger than 50 nm.

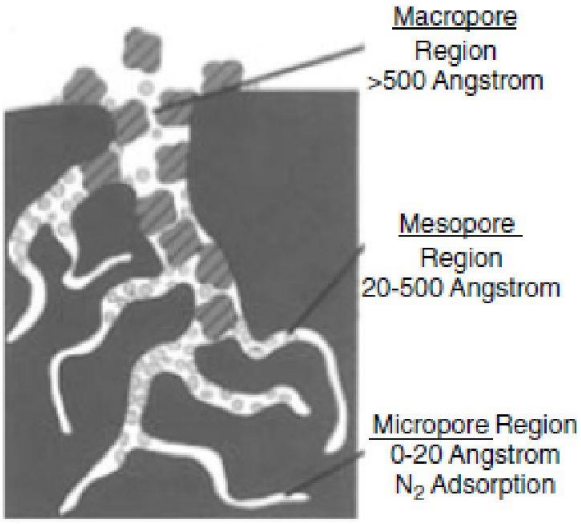

Figure 2.14 Schematic of porous regions of a sorbent [30].

CHAPTER III

EXPERIMENTAL

3.1 Materials

3.1.1 Preparation of electrospun silica nanofibers

1) Tetraethyl orthosilicate (TEOS, 98%) (Sigma-Aldrich)
2) Polyvinylpyrrolidone (PVP; 1,300,000 MW) (Sigma-Aldrich)
3) Hexadecyl-trimethyl-ammonium bromide (CTAB, 99%) (Loba Chemie)
4) Di-n-alkyl-dimethyl-ammonium chloride (DAAC, >95.0%) (TCI)
5) n-Octyl-trimethyl-ammonium bromide (OTAB, >98%) (TCI)
6) Pluronic F127 (PF) (Sigma-Aldrich)
7) Ethanol (≥ 99.9%, Merck)
8) Hydrochloric acid (37%) (Merck)

3.1.2 Adsorption of dye in water

1) Methylene blue (MB, ≥82%) (Sigma-Aldrich)
2) Ultrapure water (Milli-Q, Millipore, Germany)

3.2 Methodology

3.2.1 Critical micelle concentration (CMC) determination

CMC of surfactants in ethanol was examined using a conductivity method. The surfactant was dissolved in ethanol at concentration range of 10-70 g/L. The conductance values were plotted against the surfactant concentration and the intersection of two straight lines in the graph was calculated as the CMC value.

3.2.2 Preparation of electrospun silica nanofibers

Initially, surfactant was dissolved in ethanol (10.00 mL) and stirred at room temperature for 1 hour. Then, TEOS (1.17 mL) was poured into the solution under stirring conditions for another 1 hour and hydrochloric acid (80 µL) as a catalyst was dropped into the mixture. After the mixture reacted overnight, PVP (1 g) was added into gel solution and stirred for 2 hours. Different concentrations (1, 2 and 3 CMC) and type of surfactant (CTAB, DAAC, OTAB and PF) were investigated, and were named as shown in Table 1. The silica nanofibers without surfactant was named Si_NF.

Table 3.1 Name of fabricated silica nanofibers with various types and concentration of surfactants.

Concentration (CMC)	Surfactant			
	CTAB	DAAC	OTAB	PF
1	Si_C-1	Si_D-1	Si_O-1	Si_P-1
2	Si_C-2	Si_D-2	Si_O-2	Si_P-2
3	Si_C-3	Si_D-3	Si_O-3	Si_P-3

The setup for electrospinning was shown in Figure 3.1. The electrospinning solution was filled in a 3-mL plastic syringe and fed to blunt stainless needle (0.8 mm ID), which connected to the anode of high voltage power supply, by a syringe pump at a flow rate of 0.75 mL/h (Prosense B.V., NE-1000, USA). Aluminum foil was wrap around rotating drum (300 rpm) as a collector, which connected to

cathode, and placed 12 cm from syringe needle. The high voltage of 21 kV was applied (power supply series 230, BERTAN, Hickville, New York, USA).

The fabricated electrospun silica nanofibers were calcined in a furnace at 0.5 ºC/min to 500 ºC and held for 3 hours. The calcined silica nanofibers were mashed and stored in a desiccator.

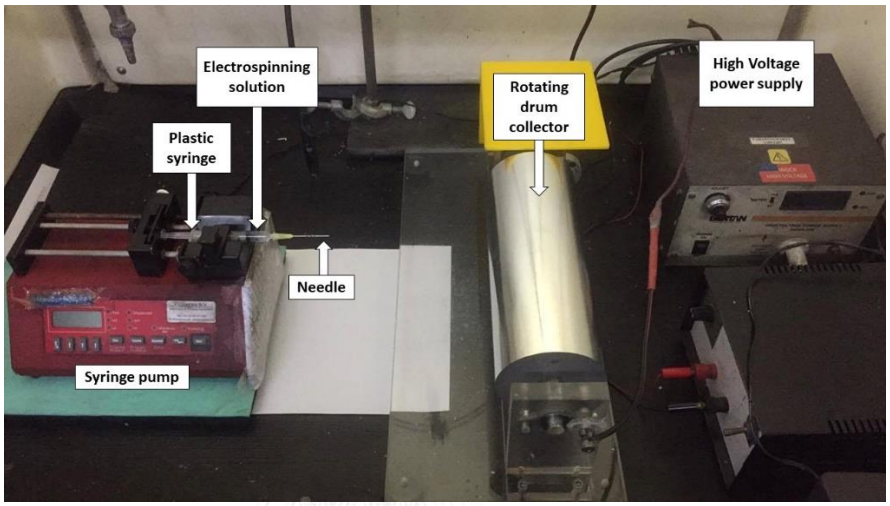

Figure 3.1 Schematic of electrospinning setup.

3.2.3 Characterization of electrospun silica nanofibers

3.2.3.1 Attenuated total reflectance Fourier-transform infrared spectroscopy (ATR-FTIR)

Silica functional groups in nanofibers were confirmed using Fourier transform infrared spectroscopy (FTIR, Nicolet 6700). A range of wavelength between 650-4000 cm^{-1} was scanned with the number of scans at 16.

3.2.3.2 Scanning electron microscope (SEM)

The surface morphologies and size of electrospun silica nanofibers were examined using a scanning electron microscope (SEM, JSM-6610LV and JSM-6400). The size of 20 nanofibers per picture were measured from SEM micrograph by ImageJ software as the average values with standard deviation.

3.2.3.3 Transmission electron microscope (TEM)

The porous morphologies in electrospun silica nanofibers were investigated by transmission electron microscope (JEM-2100 and HITACHI 770).

3.2.3.4 Nitrogen physisorption measurement

Surface area and porous properties of electrospun silica nanofibers were characterized by Brunauer, Ennett and Teller technique (BET) theory (Belsorp-mini II). The nanofibers were pre-treated at 200ºC for 2 hours.

3.2.4 Adsorption of methylene blue in water using fabricated electrospun silica nanofibers

3.2.4.1 Preparation of methylene blue solution

Six concentrations of methylene blue solution, 0.5, 1, 2, 3, 4 and 5 mg/L, were prepared in MilliQ water for calibration curve. In adsorption study, 15 mg/L methylene blue in MilliQ water was used as initial concentration.

3.2.4.2 Adsorption of methylene blue

The produced silica nanofibers were studied for the efficiency in removal of methylene blue in aqueous solutions. In all experiments, 5 mL of 15 mg/L methylene blue was added in 20 mL vial containing 5 mg of electrospun silica nanofibers. The mixtures were shaken at 100-110 rpm for 45 minutes. The solution was centrifuged at 3500 rpm for 10 minutes to separate the sorbent from aqueous phase. UV-visible at 664 nm was used to determine the residual dye concentration in the solution.

The amount of dye uptake by the adsorbent is calculated using this equation:

$$q_e \text{ (mg/g)} = (C_0 - C_e) \times V / M$$

where q_e is the amount of dye loaded on per unit of adsorbent, C_0 (mg/L) is the initial dye concentration, C_e (mg/L) is the dye concentration at equilibrium, V (L) is the volume of dye solution, and M (g) is the mass of sorbent.

The percentage of dye removal is calculated using this equation:

Dye removal (%) = $[(C_0-C_e)/ C_0] \times 100$

The effect of contact time in adsorption process was examined using silica nanofibers without surfactant (Si_NF) as a sorbent and 15 ppm methylene blue in MilliQ water as initial solution.

CHAPTER IV
RESULTS AND DISCUSSION

4.1 CMC values of surfactant

Critical micelle concentration (CMC) of surfactants in ethanol was examined using a conductivity method. The conductance of surfactant was measured and the calculated CMC is shown in Table 4.1. CTAB has the highest CMC followed by OTAB, PF, and DAAC respectively. Even though CMC should decrease with increasing tail length because of an increase of hydrophobic character [31], CMC of CTAB is slightly higher than that of OTAB. It might be the result from a steric effect. Therefore, OTAB which has least steric effect can form micelle easier than CTAB resulting in a lower value of CMC.

Table 4.1 CMC values of studied surfactants.

Surfactant	CTAB	DAAC	OTAB	PF
CMC (g/L)	20.02	8.18	17.00	9.08

On the other hand, CMC values of PF and DAAC are much lower than those of CTAB and OTAB. This might be due to their different forms of micelle or their long double alkyl chain which decrease the solubility in solvent. With the lower solubility, micelle can form easier and result in a lower value of CMC for both PF and DAAC.

4.2 Characterization of electrospun silica nanofibers

After the silica nanofibers were obtained, the characteristics were studied by FTIR, SEM, TEM, and nitrogen adsorption/desorption techniques.

4.2.1 Fourier transform infrared spectroscopy (FTIR)

After calcination, IR spectra were examined for the silanol functional group in nanofibers and the elimination of all polymer and surfactant. The fabricated silica nanofibers at 3 CMC of surfactant (highest concentration) after calcination spectra were compared with those before calcination, PVP, and surfactant spectra as shown in Figure 4.1.

Before calcination, the bands at around 1700 cm^{-1} which interpreted of ketone in PVP and the bands at around 2800 cm^{-1} which interpreted of C-H stretch in surfactant were existed. But after calcination, all the bands of PVP and surfactants were eliminated. Only the characteristic bands of SiO_2, near 1000 and 800 cm^{-1} [32], were observed after calcination as shown in Figure 4.1. Moreover, the spectra of all fabricated nanofibers were similar to the spectra of silica gel, Figure 4.2. This approved that the fabricated nanofibers are SiO_2.

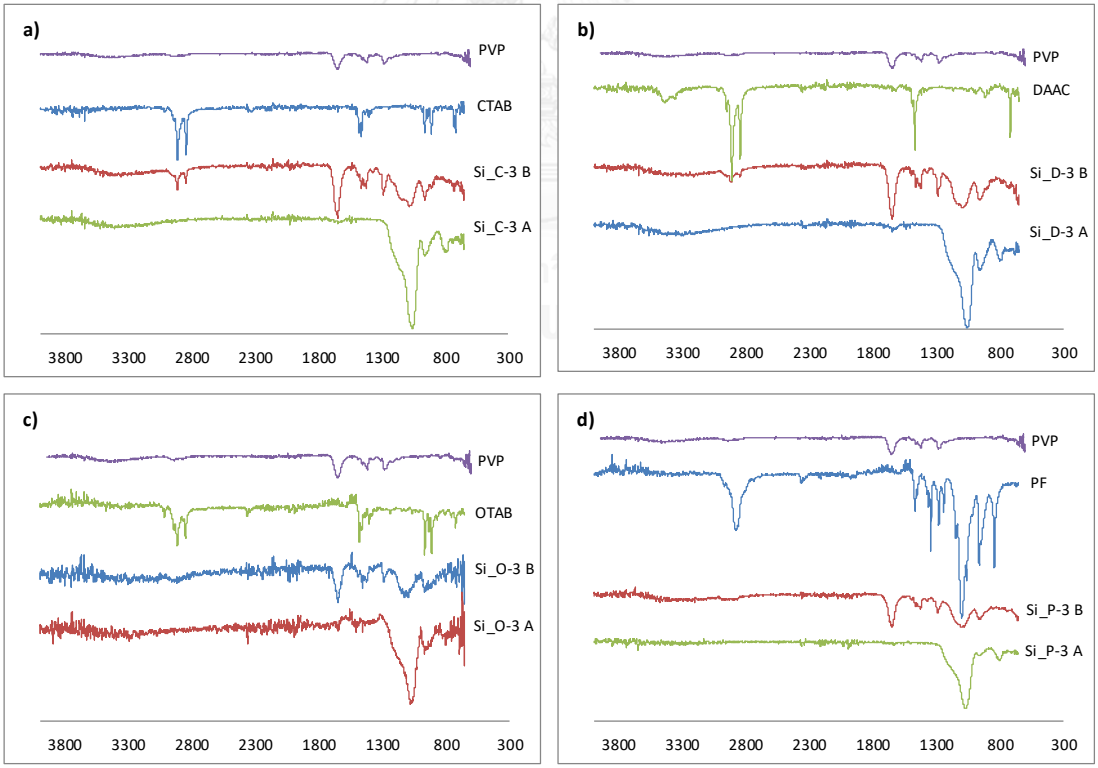

Figure 4.1 IR spectra of fabricated silica nanofibers B (before calcination) and A (after calcination) compared with PVP and surfactant spectra: a) Si_C-3, b) Si_D-3, c) Si_O-3, and d) Si_P-3.

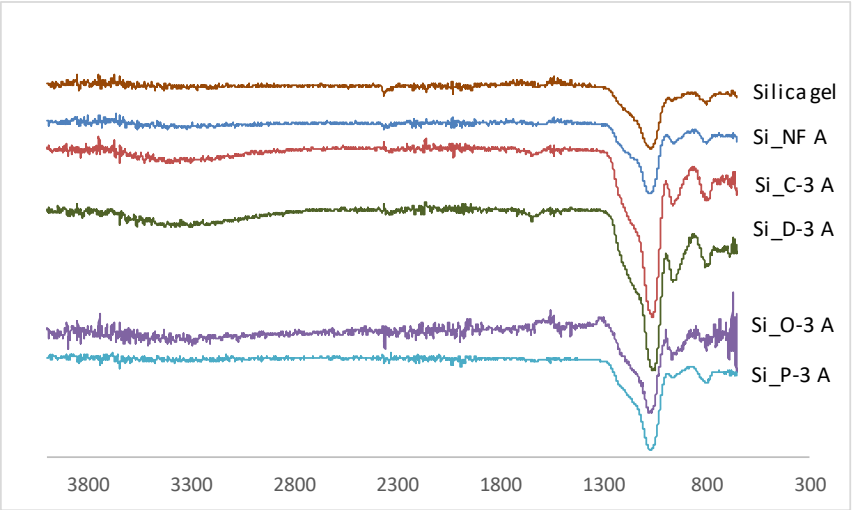

Figure 4.2 IR spectra of fabricated silica nanofibers (with 3 CMC of surfactant) after calcination compared with spectra of silica gel.

4.2.2 Scanning electron microscope (SEM)

The silica nanofibers were prepared via sol-gel reaction and electrospinning and examined the morphologies before and after calcination via SEM technique. The sol-gel reaction was set for 1-night before electrospinning. However, the silica nanofibers were not successfully prepared at high amount of OTAB. The linked-nanofibers were observed both before and after calcination as shown in Figure 4.3 which is the SEM images of silica nanofibers with 2 CMC of OTAB and sol-gel for 1-night. As a result, the sol-gel reaction containing OTAB was assumed incomplete. The OTAB surfactant might be interrupt a sol-gel process. Because OTAB is a small cationic surfactant, it may have a strong interaction with silica species during hydrolysis reaction and can slowed the condensation reaction. Therefore, the sol-gel reaction was extended to 2-nights when preparing the silica nanofibers with OTAB surfactant.

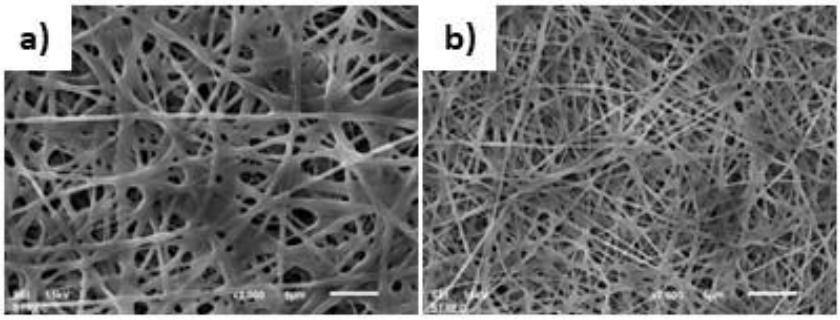

Figure 4.3 SEM images of silica nanofibers with 2 CMC of OTAB 2-nights sol-gel reaction: a) before calcination, and b) after calcination.

The morphologies of silica nanofibers before and after calcination were observed via SEM technique. Figure 4.4 and Figure 4.5 show the SEM images of silica nanofibers before and after calcination, respectively with various amount of CTAB, DAAC, OTAB and PF surfactants (1, 2 and 3 CMC). All produced silica nanofibers were smooth before calcination but became smaller and distorted after calcination.

The average fibers diameters for each silica nanofibers are summarized in Table 4.2.

Table 4.2 Average fiber diameters of silica nanofibers with different surfactant. (n=20)

Surfactant	Silica nanofibers	Average nanofibers diameters (nm)	
		Before calcined	After calcined
-	Si_NF	354±61	231±32
CTAB	Si_C-1	623±104	337±54
	Si_C-2	602±124	343±70
	Si_C-3	568±72	317±47
DAAC	Si_D-1	394±53	310±51
	Si_D-2	391±64	263±48
	Si_D-3	1942±1041	501±118
OTAB	Si_O-1	575±73	303±57
	Si_O-2	863±243	718±91
	Si_O-3	1211±277	572±84
PF	Si_P-1	1081±148	680±93
	Si_P-2	401±69	254±40
	Si-_P-3	527±107	343±49

Surfactant	Concentration of surfactant		
	1 CMC	2 CMC	3 CMC
CTAB	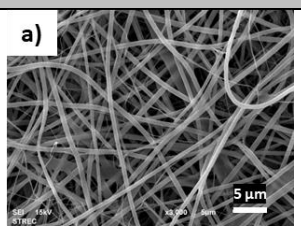	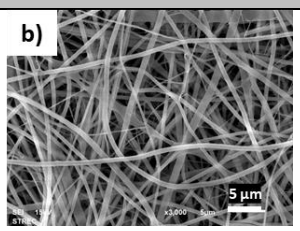	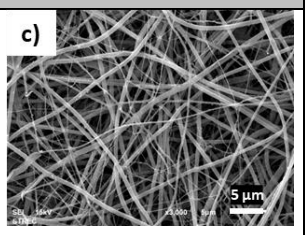
OTAB	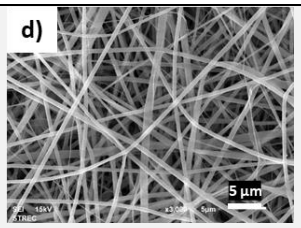	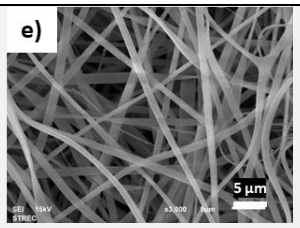	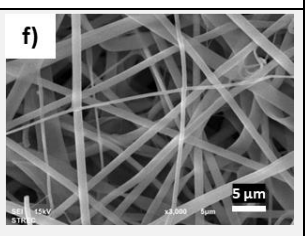
DAAC	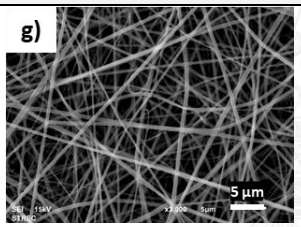	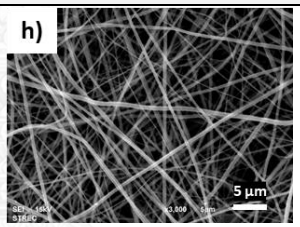	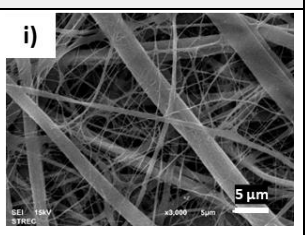
PF	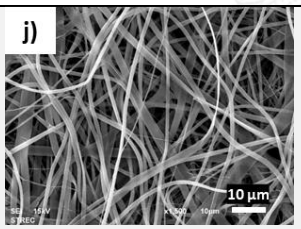	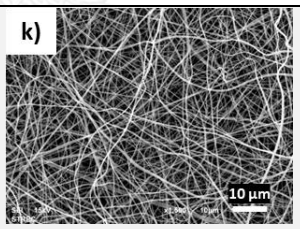	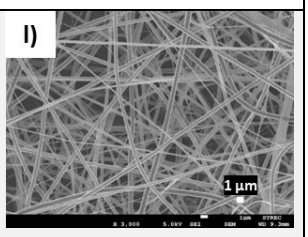

Figure 4.4 SEM images of silica nanofibers before calcination with various amount of surfactants: a) Si_C-1, b) Si_C-2, c) Si_C-3, d) Si_O-1, e) Si_O-2, f) Si_O-3, g) Si_D-1, h) Si_D-2 i) Si_D-3, j) Si_P-1, k) Si_P-2, and l) Si_P-3.

Surfactant	Concentration of surfactant		
	1 CMC	2 CMC	3 CMC
CTAB	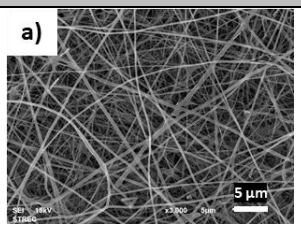	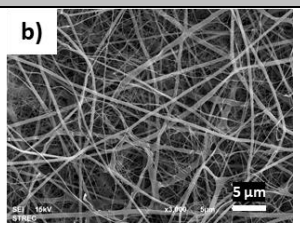	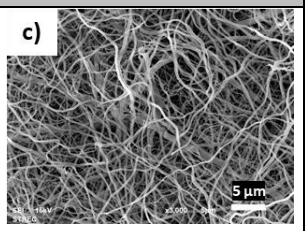
OTAB	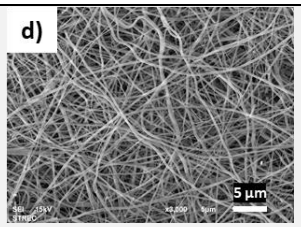	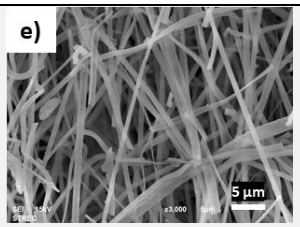	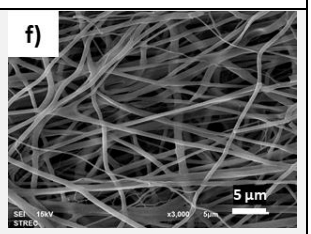
DAAC	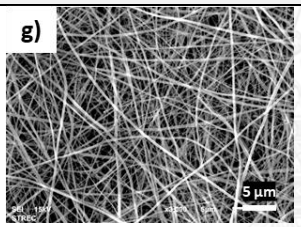	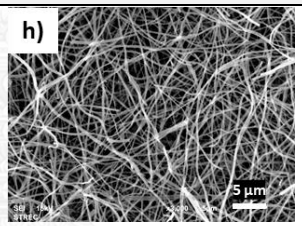	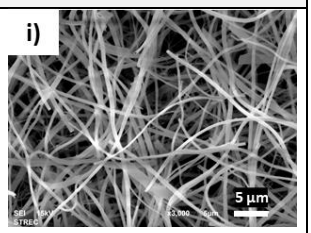
PF	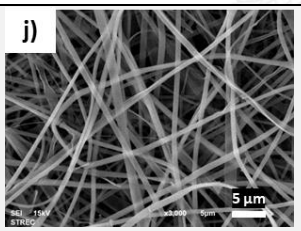	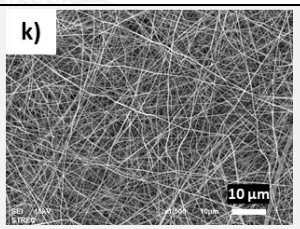	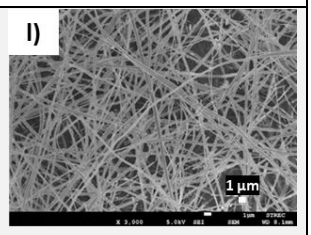

Figure 4.5 SEM images of silica nanofibers after calcination with various amount surfactants: a) Si_C-1, b) Si_C-2, c) Si_C-3, d) Si_O-1, e) Si_O-2, f) Si_O-3, g) Si_D-1, h) Si_D-2 i) Si_D-3, j) Si_P-1, k) Si_P-2, and l) Si_P-3.

For CTAB surfactant, the silica nanofibers were fine and smooth both before and after calcination. However, the silica nanofibers were smaller and slightly distorted after calcination. The average diameter of nanofibers before calcination was 568-623 nm and 317-343 nm after calcination. Notably, the fiber diameters with various amount of surfactant are not different. Nevertheless, the decrease of fiber diameter and the distortion of nanofibers after calcination might cause from the collapse of nanofiber structure when PVP and surfactant were eliminated in calcination process.

For OTAB surfactant, like the others, the silica nanofibers were smaller after calcined (576-1211 nm before calcination to 303-719 nm after calcination). Before calcination, the size of silica nanofibers was slightly increased with increasing the amount of surfactant. However, the size of silica nanofibers after calcination with various amount of OTAB was quite similar, accept Si_O-1 which is thinnest.

For DAAC surfactant, the obtained silica nanofibers were similar to those of CTAB surfactant except at 3 CMC. The average diameter of nanofibers with 1 CMC and 2 CMC were 394 and 391 nm before calcination and 310 nm and 263 nm after calcination. The silica nanofibers with 3 CMC was irregular before calcination. The regular of fibers were better after calcination and average diameter of nanofibers was 501 nm.

For PF surfactant, the surface of nanofibers was smooth and the size of nanofibers was smaller after calcination (527-1082 nm before calcination to 254-680 nm after calcination). Moreover, size of silica nanofibers was decrease with increasing amount of surfactant from 1 CMC to 2 CMC. But when increase the amount of PF surfactant from 2 CMC to 3 CMC, the size of nanofibers was not significantly increase.

4.2.3 Transmission electron microscope (TEM)

The porous structure inside silica nanofibers were observed via TEM technique. According to Galarneau et al.'s research [33], the mesoporous and meso-/macroporous silica monoliths were synthesized. They found that when the low concentration of polymer was used, the polymer can form micelle with hydrophobic part at the micelle core and hydrophilic part at the surface interact with silica environment. Concurrently, the condensation of silica will occur around the polymer micelle, result in ordered mesoporous structure when the polymer was removed as shown in Figure 4.6.

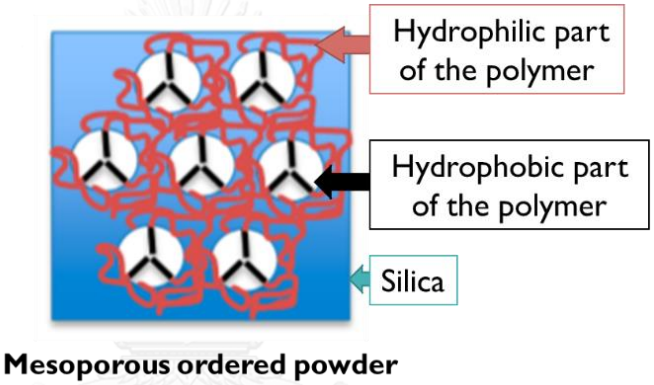

Figure 4.6 Schematic represent of the mesoporosity of the materials. [33]

Therefore, in this research, we expect that the cationic or polar group of surfactants may interact strongly with silica species by electrostatic force, at pH>2 silica species are deprotonated and become negative charge [34], and complexes of silica/surfactant were formed. After that, the hydrophobic groups of surfactants will interact to form micelle under silica condensation and self-assembly mechanism was occurred, as illustrated in Figure 4.7.

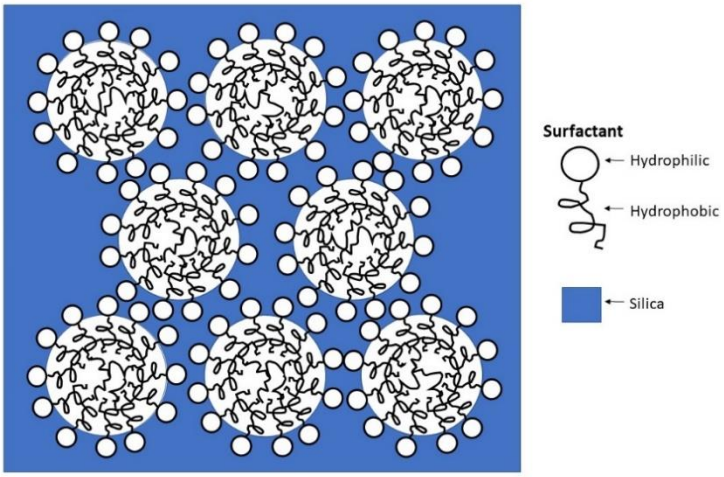

Figure 4.7 Schematic representation of porosity in silica nanofibers. Reproduced from ref. [33].

As a result, mesoporous silica materials would observe when surfactants were removed. Nonetheless, the mesoporous structure in silica nanofibers cannot be observed in all concentration of CTAB and OTAB which are shown in Figure 4.8 a)- c) and Figure 4.8 d)- f). It implied that the micelle size of CTAB and OTAB, which have single long and short non-ionic chain, might be too small and then form microporous structure in silica network instead of mesoporous or macroporous structure.

Surfactant	Concentration of surfactant		
	1 CMC	2 CMC	3 CMC
CTAB	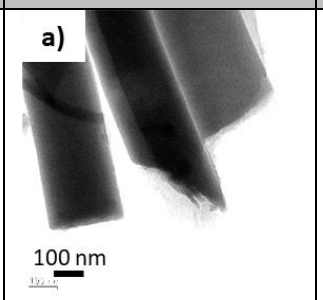	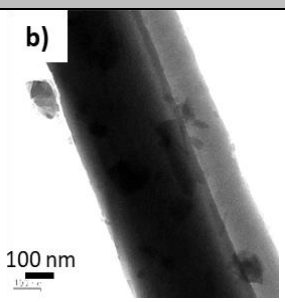	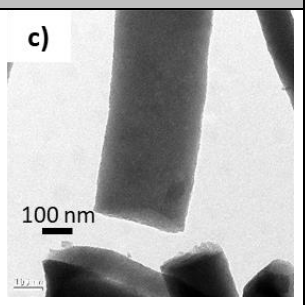
OTAB	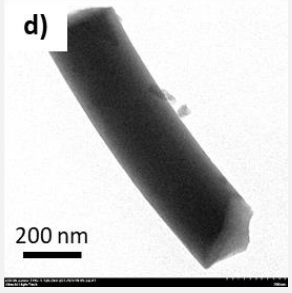	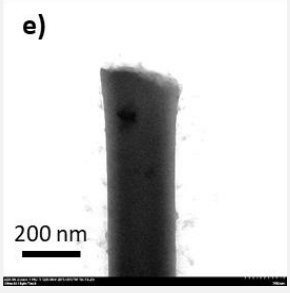	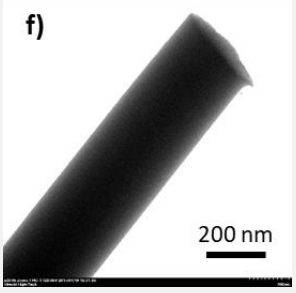
DAAC	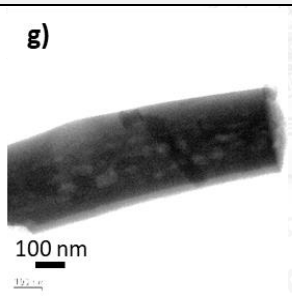	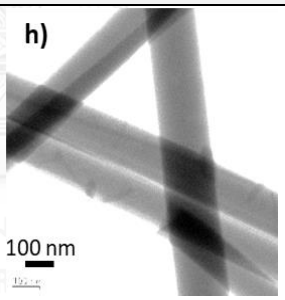	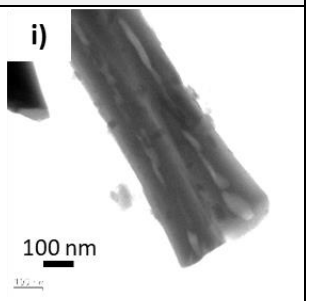
PF	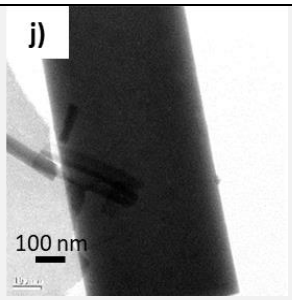	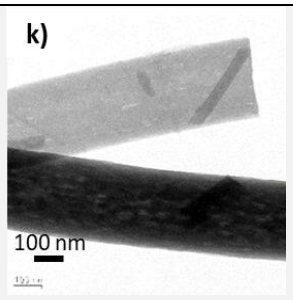	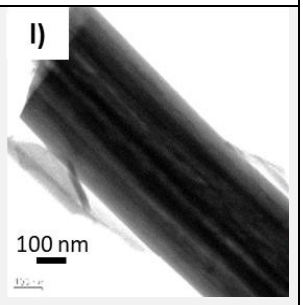

Figure 4.8 TEM images of silica nanofibers a) Si_C-1, b) Si_C-2, c) Si_C-3, d) Si_O-1, e) Si_O-2, f) Si_O-3, g) Si_D-1, h) Si_D-2 i) Si_D-3, j) Si_P-1, k) Si_P-2, and l) Si_P-3.

However, TEM images of silica nanofibers with DAAC surfactant in Si_D-1 and Si_D-3 (Figure 4.8 g) and 4.8 i)) were noticed a mesoporous structure while mesoporous structure was not noticed in Si_D-2. It assumed that DAAC surfactant can also interact and form complexes with silica species via electrostatic interaction. Then, silica condensation and self-assembly mechanism were taken place and mesoporous structure was formed. However, micelle of DAAC, which have two non-ionic chains, in Si_D-1 might form in spherical and elliptical shape that big enough to form mesoporous structure. As a result, spherical and elliptical shape mesoporous structure was observed as shown in Figure 4.8 g).

At 2 CMC of DAAC (Si_D-2), micelles might change into another form which were too small to form mesoporous structure as Si_D-1. But the Si_D-2 nanofibers were rather thin, implied that there were large number of small micelle to act as porous template in the fibers. Unfortunately, porous structure was observed again in Si_D-3 with higher amount of DAAC. This presumed that DAAC micelles transform to rod or ellipsoid shape when the concentration of DAAC increases.

Similarly, porous structure can be observed in silica nanofibers with PF surfactant at 2 and 3 CMC, Figure 4.8 k) and 4.8 l). Porous structure was not observed at 1 CMC of PF surfactant, assumed that the micelle of surfactant at 1 CMC was too small to form mesoporous structure. Porous structure in Si_P-2 was sphere, and in Si_P-3 was cylinder. According to Lu Han and Shunai Che's research [34], cationic surfactant can interact with silica species and the hydrophobic part of surfactant were induced to from the helical propeller-like configuration in rod-like micelles as shown in Figure 4.9. Then the rod-like porous structure were built after the surfactant was removed. Rod-like porous structure was seen in Si_P-3. Therefore, hydrophilic group of PF surfactant at 3 CMC might be interacted with silica species and build a rod-like micelle. Whereas PF is non-ionic surfactant, the interaction between two hydrophilic tail of PF and silica species might be H-bond or dipole-dipole interaction.

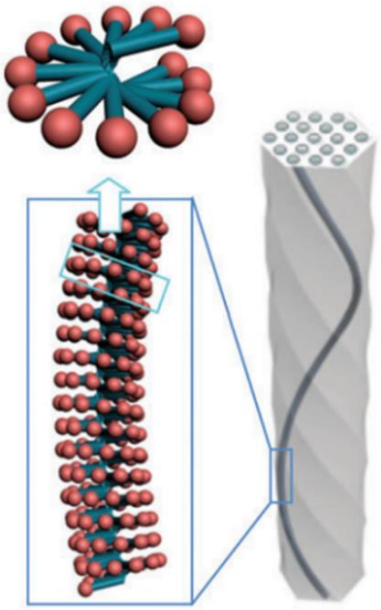

Figure 4.9 Molecular origin of helical mesostructure of chiral mesoporous silica derived from the helical packing of chiral amphiphiles [34].

4.2.4 N_2 adsorption/desorption

The porous characteristics of the silica nanofibers with different surfactants were studied for adsorption/desorption isotherm as shown in Figure 4.10. All the nitrogen adsorption/desorption isotherms of fabricated nanofibers are type I, microporous solids [35]. In addition, the surface area, pore volume and mean pore diameter of obtained silica nanofibers calculated are summarized in Table 4.3.

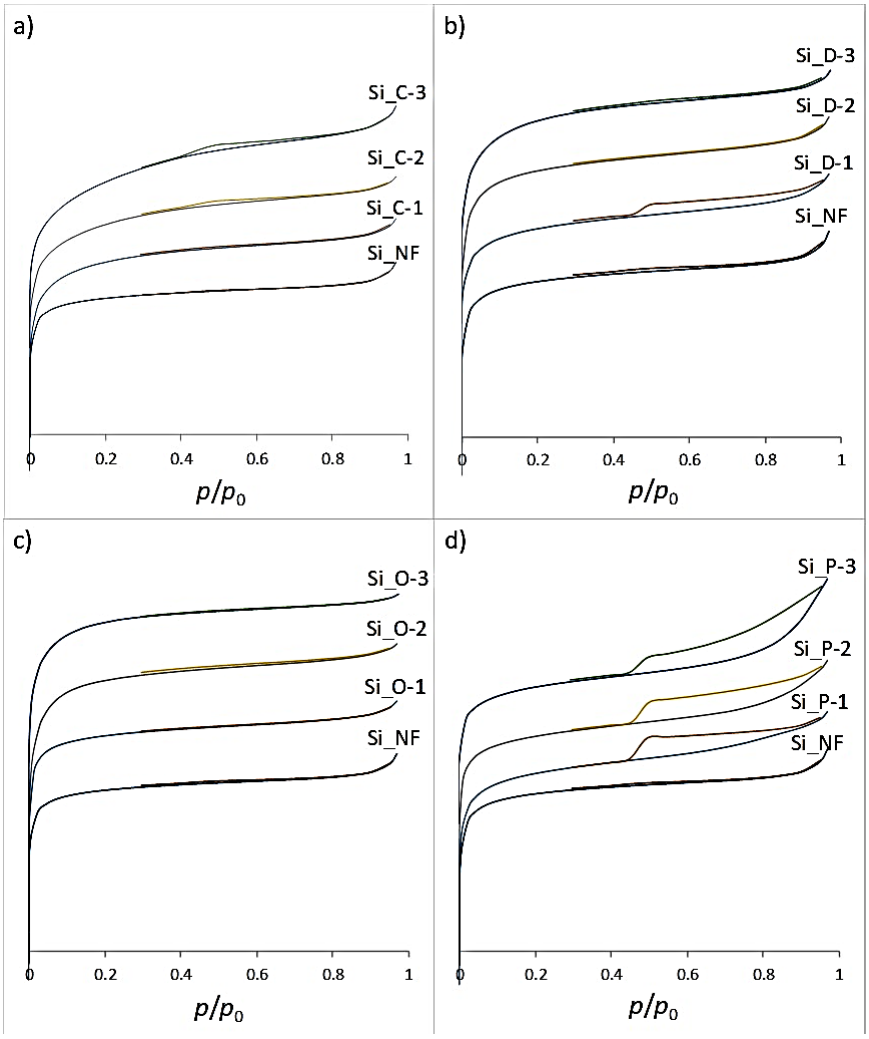

Figure 4.10 Nitrogen adsorption/desorption isotherm of silica nanofibers a) Si_C, b) Si_D, c) Si_O, and d) Si_P compared with Si_NF.

Table 4.3 Data from nitrogen adsorption/desorption technique.

Surfactants	Nanofibers	Surface area (m^2/g)	Pore volume (cm^3/g)	Pore diameter (nm)
-	Si_NF	399.12	0.20	2.02
CTAB	Si_C-1	564.32	0.27	1.94
	Si_C-2	478.98	0.24	2.04
	Si_C-3	443.24	0.26	2.38
OTAB	Si_O-1	627.87	0.28	1.79
	Si_O-2	778.46	0.35	1.80
	Si_O-3	670.12	0.30	1.82
DAAC	Si_D-1	499.92	0.24	1.92
	Si_D-2	599.62	0.28	1.86
	Si_D-3	558.54	0.26	1.89
PF	Si_P-1	495.57	0.25	1.98 2.15*
	Si_P-2	451.36	0.24	2.11 2.49*
	Si-_P-3	342.01	0.22	2.62 4.48*

*The pore diameter calculated using t-plot method.

The H4 type hysteresis loops, which refers to uniform of porous size and/or shape [35], in Si_C nanofibers were observed at high amount of CTAB (2 and 3 CMC). Therefore, an increase of CTAB causes the porous size and/or shape more uniform. Moreover, the surface area and pore volume decrease with an increase of amount of CTAB. Meanwhile the pore diameter increases with an increase of amount of CTAB. It is assumed that the size of CTAB micelle will increases and the number of micelle will decrease as the concentration of CTAB surfactant is increase. Therefore, with bigger size and less number of micelle, the surface area and pore volume of Si_C decreased.

Among the various type of surfactant, the Si_O nanofibers gave the highest surface area. Meanwhile, the amount of OTAB almost does not affect the nitrogen adsorption/desorption isotherm. Pore diameters of Si_O are nearly the same. Although their pore diameters are equal, Si_O-2 have the large pore volume. It is assumed that the number of OTAB micelle will increase with an increase of OTAB concentration, which leads to larger pore volume and higher surface area.

For DAAC surfactant, hysteresis loops of silica nanofibers were decrease with increasing amount of DAAC. Even though, Si_D-1 was the most uniform porous, Si_D-1 has least surface area among Si_D nanofibers. However, the pore diameters of all Si_D nanofibers were almost the same which disagree with TEM images that mesoporous structure can be observed in Si_D-1 and Si_D-3. This presumed that the mesoporous in Si_D-1 and Si_D-3 are dominated by microporous in nanofibers, so the diameter calculated from N_2 adsorption/desorption isotherm showed the microporous size.

Unlike the others, isotherm of Si_P nanofibers show H3 type hysteresis loop at all amount of PF surfactant, refers to their nonuniform porous. Si_P-3 nanofibers gave the biggest pore diameter and least surface area, due to the big porous tube along the length of nanofibers as shown in Figure 4.6. However, the pore size of Si_P were not different from the size of microporous in other nanofibers, even if the mesoporous were clearly noticed in TEM images. Therefore, t-plot method was applied to determined pore size in Si_P nanofibers.

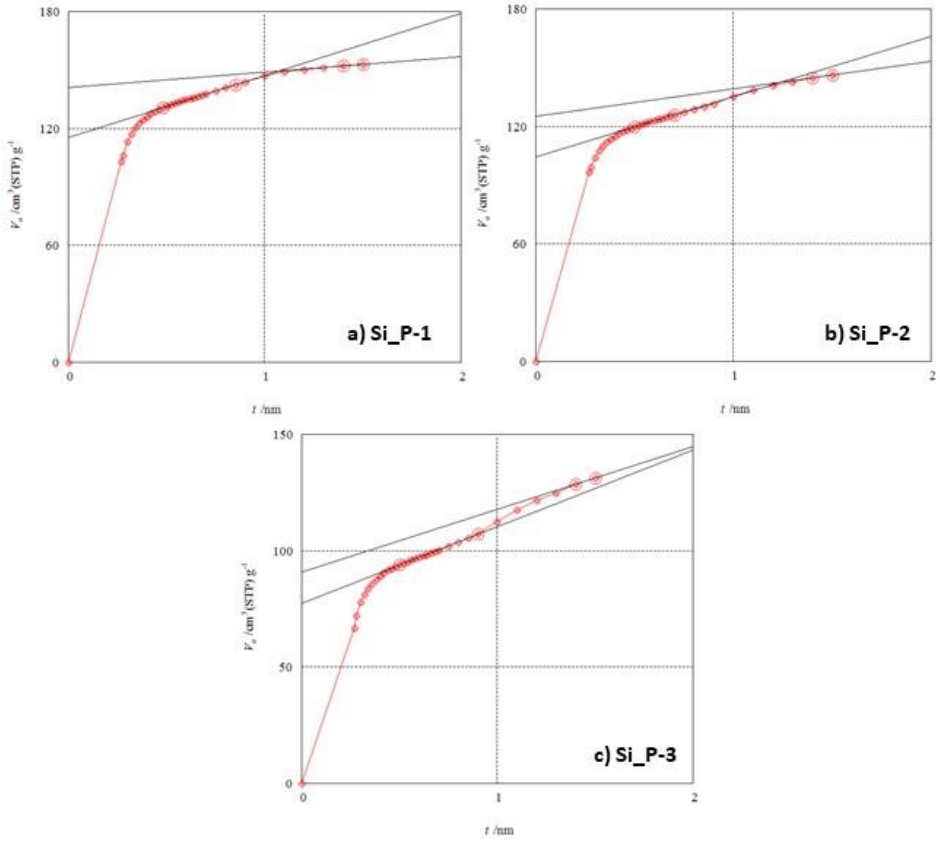

Figure 4.11 t-plot of silica nanofibers with PF surfactant: a) Si_P-1, b) Si_P-2, and c) Si_P-3.

According to Figure 4.11, t-plot of Si_P slightly show pattern of mesoporous type and larger pore diameters, which is consistent with TEM images. Therefore, the pore diameter of Si_P nanofibers were calculated from t-plot method. As a result, the porous size increased with an increase of PF surfactant concentration. It is assumed that the size of PF micelle will increases when the concentration of PF surfactant increase.

In comparison of isotherm with Si_NF nanofibers shown in Figure 4.10, some of fabricated silica nanofibers show an increase in uniform porous structure. It assumed that the addition of surfactant at different concentration can affect the formation of silica network structure. An increase of CTAB concentration can slightly improve the uniform of porous, while an increase of DAAC decreases a porous uniform. On the other hands, OTAB surfactant does not affect an uniformity of porous structure

at all, possibly due to the small size of OTAB micelle. Moreover, the addition of PF surfactant showed nonuniform porous structure.

4.2.5 Morphologies of fabricated electrospun silica nanofibers

From Table 4.4, the mopgologies and characteristics of fabricated electrospun silica nanofibers were compared.

Table 4.4 The electrospun silica nanofibers morphologies.

Surfactant	None	CTAB			OTAB			DAAC			PF		
Concentration (CMC)		1	2	3	1	2	3	1	2	3	1	2	3
Mesoporous shape (TEM image)	-	-			-			○	-	▯	-	○	▯
Mean pore diameter (nm)	2.0	1.9	2.0	2.4	1.8	1.8	1.8	1.9	1.9	1.9	2.2	2.5	4.5
Surface area (m^2/g)	399	564	479	443	628	778	670	500	600	558	496	451	342
Adsorption/ desorption isotherm	Microporous	Microporous			Microporous			Microporous + Mesoporous (in Si_D-1)			Microporous + Mesoporous		

According to the adsorption/desorption isotherm, most of fabricated silica nanofibers were type I or microporous solids. Agreeable with the assumption of microporous structure in silica nanofibers with CTAB and OTAB surfactant. The isotherm of Si_P nanofibers slightly showed the pattern of a mesoporous type isotherm. It is assumed that the microporous structure was dominate over mesoporous structure, so the isotherms were shown in microporous type instead of mesoporous type. On the other hand, the isotherms of Si_D nanofibers were shown in both microporous and micro-/mesoporous type. Even though both Si_D-1 and Si_D-3 showed mesoporous

structure, Si_D-3 isotherm was only microporous while Si_D-3 isotherm was microporous with slightly of mesoporous type similar to the isotherm in Si_P. It presumed that the formation of micelle in Si_D-1 might similar to those in Si_P. Also, the formation of micelle in Si_D-3 might similar to those in Si_C and Si_O.

In addition, the mesoporous structure was observed in silica nanofibers with steric structure of surfactant. The mesoporous structure was present in Si_D-1, Si_D-2, Si_P-2, and Si_P-3 nanofibers with different porous shapes. The nanofibers with lower concentration of surfactant showed spherical or elliptical porous shape. While the nanofibers with higher concentration of surfactant showed cylindrical or rod-like porous shape. It assumed that the hydrophobic chain of surfactant may induced the surfactant to form rod-like micelle and then leading to a helical structure along the length of nanofibers.

Additionally, the pore size of nanofibers is related to the surfactant micelle size. The pore diameter of Si_C was larger than Si_O because CTAB contains a longer alkyl chain. So, a micelle of CTAB was bigger than a micelle of OTAB which leading to larger pore diameter.

When the pore diameter of Si_C and Si_D were compared, the pore diameter of Si_C was larger than that of Si_D although the size of DAAC surfactant, which have double non-ionic chains, is bigger than CTAB surfactant, which have a single non-ionic chain. It assumed that micelle of DAAC was smaller than that of CTAB. Besides, CMC values of CTAB is much higher than that of DAAC. Therefore, DAAC can form micelle at a lower concentration. Unlike CTAB, micelle was formed at high concentration. It assumed that the micelle size of CTAB might be bigger than DAAC because of larger number of molecules of CTAB in micelle structure.

The surfactants with high steric structure, DAAC and PF, can produced mesoporous in nanofibers. While the interaction between cationic surfactant and silica species is electrostatic interaction, the interaction between silica species and PF is dipole-dipole interaction. The interaction of PF might not as strong as the interaction of DAAC. So, the pore size in Si_P nanofibers was bigger than in Si_D nanofibers because

PF might likely form micelle more than interact with silica species, leading to a big and steady porous structure in Si_P.

In comparison to the commercial silica gel, the surface area of fabricated electrospun silica nanofibers were higher than the commercial silica gel. This implied that electrospinning technique can provide high surface area materials. Moreover, surface area of nanofibers with surfactant were higher than nanofibers without surfactant. This approved that the addition of surfactant can provide porous structure in electrospun silica nanofibers and can improve surface area.

4.3 Adsorption of methylene blue (MB) in water

The fabricated nanofibers were applied as an adsorbent to remove MB in water. Typically, surface of silica nanofibers is negative charge, when pH>2, and can adsorb cationic species, like MB, by electrostatic attraction [36]. After the adsorption, MB solution which has blue color turned into pale blue to almost clear depend on the amount of dye that can be uptake in silica nanofibers.

From Figure 4.12, the results showed that all fabricated silica nanofibers have high efficiency in MB adsorption and higher than the commercial silica gel. This implied that silica nanofibers provided higher surface area and appropriate in adsorption application. The silica nanofibers without the addition of surfactant, Si_NF, showed the lowest efficiency in MB removal from water. This can be proved that the addition of surfactant can increase surface area of silica nanofibers.

According to their surface area, Si_O-2 has the highest surface area, which is agreeable with the highest efficiency in MB adsorption. However, the efficiency of fabricated silica nanofibers with different surfactants in MB adsorption is not dramatically different. The percentages of MB removal were 88-97% which was agreeable with their surface area.

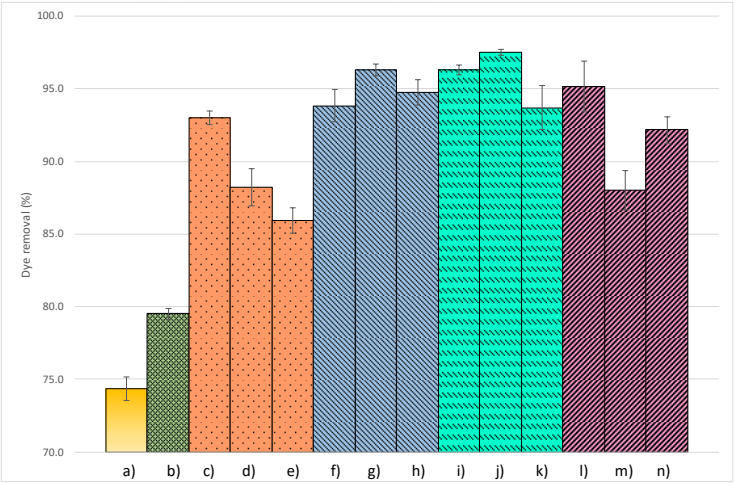

Figure 4.12 Removal value (%) of methylene blue when used fabricated silica nanofibers a) silica gel, b) Si_NF, c) Si_C-1, d) Si_C-2, e) Si_C-3, f) Si_D-1, g) Si_D-2, h) Si_D-3, i) Si_O-1, j) Si_O-2 k) Si_O-3, l) Si_P-1, m) Si_P-2, and n) Si_P-3 as adsorbent.

CHAPTER V
CONCLUSIONS

5.1 Conclusions

Electrospun silica nanofibers with porous structure were produced by electrospinning technique via sol-gel process and surfactant self-assembly. Nanofibers were distorted when high concentration of surfactants was used. In addition, high concentration of short chain surfactant, OTAB, interrupts the formation of silica network structure in sol-gel reaction, so, it needs longer time in a sol-gel process.

For cationic surfactant, the number and size of non-ionic chain slightly affect the porous formation in silica nanofibers, DAAC with double chain can provide mesoporous in silica nanofibers via surfactant self-assembly. Non-ionic surfactant with huge structure, PF, can also provide porous like DAAC. Moreover, the amount of surfactant also affects the self-assembly of surfactant micelle and leads to different shapes of porous structure.

Furthermore, four surfactants (CTAB, DAAC, OTAB and PF) showed different surface area and porous structure. The amount and type of surfactant also affected the uniformity of porous structure. Porous are more regular when increasing amount of CTAB, but worse with increasing amount of DAAC, and barely affected by varying amount of OTAB. While the porous was in nonuniform type when use PF surfactant.

Silica nanofibers showed high efficiency in dye adsorption over commercial silica gel. The addition of surfactant can improve silica nanofibers surface area which is benefit when used as adsorbent. All fabricated silica nanofibers showed high percentage of dye removal in water.

5.2 Future work

The size of some surfactants that used in this research were rather small, so the formation of mesoporous were difficult. Only the surfactant with huge or high steric structure, like DAAC and PF, can created the mesoporous structure. Therefore, more surfactants, both cationic and non-ionic surfactants, with huge structure and high steric structure should be studied in different concentration. The chain part of surfactant, hydrophobic and hydrophilic, also should be studied. To confirmed the effect of surfactant type and concentration on the formation of porous structure. In order to design electrospun silica nanofibers with controlled mesoporous structure via surfactant self-assembly.

REFERENCES

[1] Wu, C., Yuan, W., Al-Deyab, S.S., and Zhang, K.-Q. Tuning Porous Silica Nanofibers by Colloid Electrospinning for Dye Adsorption. Applied Surface Science 313 (2014): 389-395.

[2] Li, S., Yue, X., Jing, Y., Bai, S., and Dai, Z. Fabrication of Zonal Thiol-functionalized Silica Nanofibers for Removal of Heavy Metal Ions from Wastewater. Colloids and Surfaces A: Physicochemical and Engineering Aspects 380(1–3) (2011): 229-233.

[3] Patel, A.C., Li, S., Wang, C., Zhang, W., and Wei, Y. Electrospinning of Porous Silica Nanofibers Containing Silver Nanoparticles for Catalytic Applications. Chemistry of Materials 19(6) (2007): 1231-1238.

[4] Lu, P.-P., Xu, Z.-L., Yang, H., and Wei, Y.-M. Preparation and Characterization of High-Performance Perfluorosulfonic Acid/SiO2 Nanofibers with Catalytic Property via Electrospinning. Industrial & Engineering Chemistry Research 51(35) (2012): 11348-11354.

[5] Hou, Z., et al. Luminescent Porous Silica Fibers as Drug Carriers. Chemistry 16(48) (2010): 14513-9.

[6] Zong, X., et al. Fabrication and Characterization of Electrospun SiO2 Nanofibers Absorbed with Fatty Acid Eutectics For Thermal Energy Storage/retrieval. Solar Energy Materials and Solar Cells 132 (2015): 183-190.

[7] Guo, M., Ding, B., Li, X., Wang, X., Yu, J., and Wang, M. Amphiphobic Nanofibrous Silica Mats with Flexible and High-Heat-Resistant Properties. The Journal of Physical Chemistry C 114(2) (2010): 916-921.

[8] Kresge, C.T., Leonowicz, M.E., Roth, W.J., Vartuli, J.C., and Beck, J.S. Ordered Mesoporous Molecular Sieves Synthesized by A Liquid-Crystal Template Mechanism. Nature 359(6397) (1992): 710-712.

[9] He, H., Wang, J., Li, X., Zhang, X., Weng, W., and Han, G. Silica Nanofibers with Controlled Mesoporous Structure via Electrospinning: From Random to Orientated. Materials Letters 94 (2013): 100-103.

[10] Zhou, Y., Zhang, W.P., Wang, G., Zhang, Y.Q., Cao, J.H., and Wu, D.Y. Effect of Cosurfactants on Pore Sizes of Continuous Highly Ordered Mesoporous Silica Nanofibers. Applied Mechanics and Materials 597 (2014): 13-16.

[11] Nagamine, S., Kosaka, K., Tohyama, S., and Ohshima, M. Silica Nanofiber with Hierarchical Pore Structure Templated by A Polymer Blend Nanofiber and Surfactant Micelle. Materials Research Bulletin 50 (2014): 108-112.

[12] Islam, M.S., Rahaman, M.S., and Yeum, J.H. Phosphine-functionalized Electrospun Poly(vinyl alcohol)/silica Nanofibers as Highly Effective Adsorbent for Removal of Aqueous Manganese and Nickel Ions. Colloids and Surfaces A: Physicochemical and Engineering Aspects 484 (2015): 9-18.

[13] Zhao, J., Xu, X., Dong, W., and Yu, H. Self-assembly of Some Long-tail Surfactants Driven by Water Addition in Ethanol. Colloids and Surfaces A: Physicochemical and Engineering Aspects 484 (2015): 253-261.

[14] Dr. Edward Group DC, N., DACBN, DCBCN, DABFM. What Is Silica and How Can it Support Your Health? [Online]. 2016. Available from: http://www.globalhealingcenter.com/natural-health/what-is-silica-support-health/

[15] Papirer, E. Adsorption on Silica Surfaces. surfactant science. Vol. 90, 2000.

[16] Christy, A.A. The Nature of Silanol Groups on The Surfaces of Silica, Modified Silica and Some Silica Based Materials. Department of Science, Faculty of Engineering and Science University of Agder, 2014.

[17] Pandey, K. Explain How The Order of Decreasing Melting Point Is: SiO2, NaCl, Dry ice? [Online]. 2016. Available from: https://www.quora.com/Explain-how-the-order-of-decreasing-melting-point-is-SiO2-nacl-dry-ice

[18] Cerveny, S., Schwartz, G.A., Otegui, J., Colmenero, J., Loichen, J., and Westermann, S. Dielectric Study of Hydration Water in Silica Nanoparticles. The Journal of Physical Chemistry C 116(45) (2012): 24340-24349.

[19] Buckley, A.M. and Greenblatt, M. The Sol-Gel Preparation of Silica Gels. Journal of Chemical Education 71(7) (1994): 599.

[20] SHAH, A.M.K.A.S.S. Determination of Critical Micelle Concentration (Cmc) of Sodium Dodecyl Sulfate (SDS) and The Effect of Low Concentration of Pyrene

on Its Cmc Using ORIGIN Software. Journal of the Chemical Society of Pakistan 30 (2008): 186-191.

[21] Surfactant. in *Technical Brief*. 2010, Particle Sciences drug development services: 3894 Courtney Street

Bethlehem, USA.

[22] Almuhamed, S., et al. Electrospinning of PAN Nanofibers Incorporating SBA-15-type Ordered Mesoporous Silica Particles. European Polymer Journal 54 (2014): 71-78.

[23] Mi-Ra Kim, S.-H.P., Ji-Un Kim and Jin-Kook Lee. Solar Cells - Dye-Sensitized Devices. Dye-Sensitized Solar Cells Based on Polymer Electrolytes. 2011.

[24] Wang, Z.L.C. One-Dimensional Nanostructure. Effects of Working Parameters on Electrospinning SpringerBriefs in Materials, 2013.

[25] Darrell H Reneker, I.C. Nanometre Diameter Fibres of Polymer, Produced by Electrospinning. Nanotechnology. Vol. 7(3), 1996.

[26] Yuan, X., Zhang, Y., Dong, C., and Sheng, J. Morphology of Ultrafine Polysulfone Fibers Prepared by Electrospinning. Polymer International 53(11) (2004): 1704-1710.

[27] Deitzel, J.M., Kleinmeyer, J., Harris, D., and Beck Tan, N.C. The Effect of Processing Variables on The Morphology of Electrospun Nanofibers and Textiles. Polymer 42(1) (2001): 261-272.

[28] Demir, M.M., Yilgor, I., Yilgor, E., and Erman, B. Electrospinning of Polyurethane Fibers. Polymer 43(11) (2002): 3303-3309.

[29] Haghi, A.K. and Akbari, M. Trends in Electrospinning of Natural Nanofibers. physica Status Solidi (a) 204(6) (2007): 1830-1834.

[30] Chigome, S. and Torto, N. Electrospun Nanofiber Based Solid Phase Extraction. in Maguire, R. (ed.)Advances in Nanofibers, p. Ch. 01. Rijeka: InTech, 2013.

[31] Mandavi, R. Kinetic Studies of Some Esters and Amides in Presence of Micelles. Chemistry Pt. Ravishankar Shukla University, 2011.

[32] Hanna, R. Infrared Absorption Spectrum of Silicon Dioxide. Journal of the American Ceramic Society 48(11) (1965): 595-599.

[33] Galarneau, A., et al. Synthesis and Textural Characterization of Mesoporous and Meso-/Macroporous Silica Monoliths Obtained by Spinodal Decomposition. Inorganics 4(2) (2016): 9.

[34] Qiu, H. and Che, S. Chiral Mesoporous Silica: Chiral Construction and Imprinting via Cooperative Self-assembly of Amphiphiles and Silica Precursors. Chemical Society Reviews 40(3) (2011): 1259-1268.

[35] Leofanti, G., Padovan, M., Tozzola, G., and Venturelli, B. Surface Area and Pore Texture of Catalysts. Catalysis Today 41(1–3) (1998): 207-219.

[36] Huang, C.-H., Chang, K.-P., Ou, H.-D., Chiang, Y.-C., and Wang, C.-F. Adsorption of Cationic Dyes onto Mesoporous Silica. Microporous and Mesoporous Materials 141(1–3) (2011): 102-109.

APPENDIX

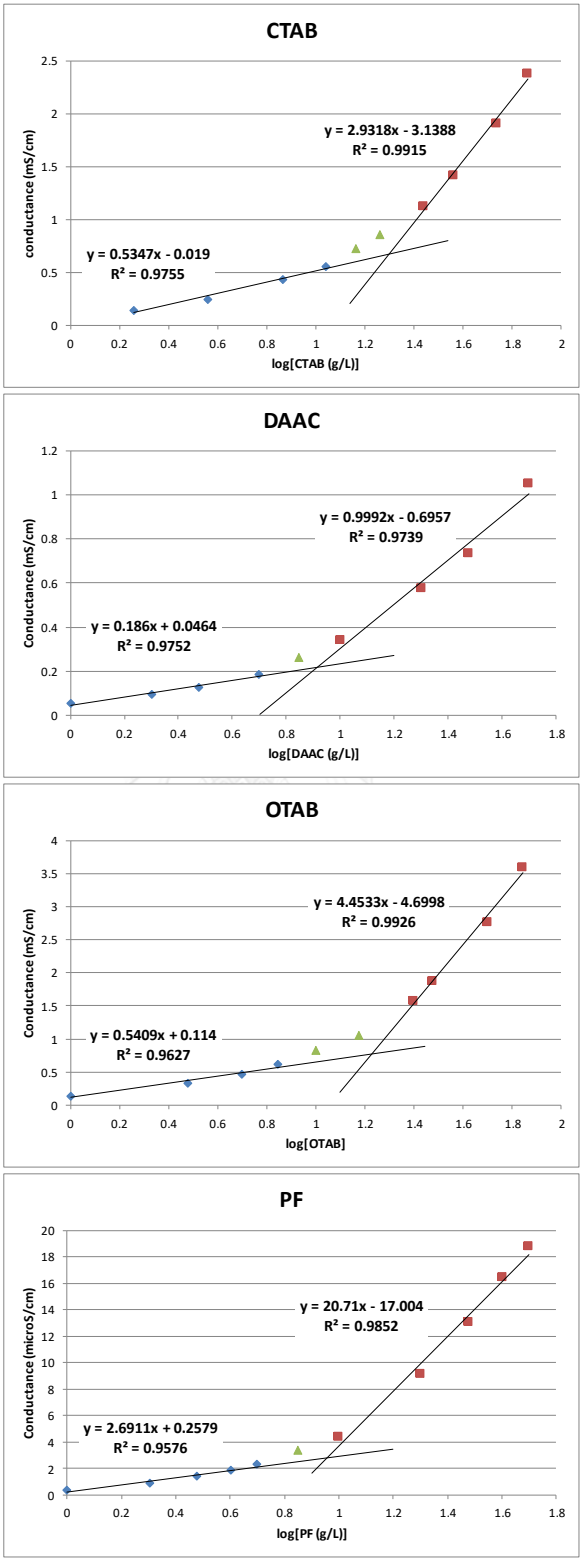

Figure A-1 Plot of conductivity versus varying concentrations of surfactants.

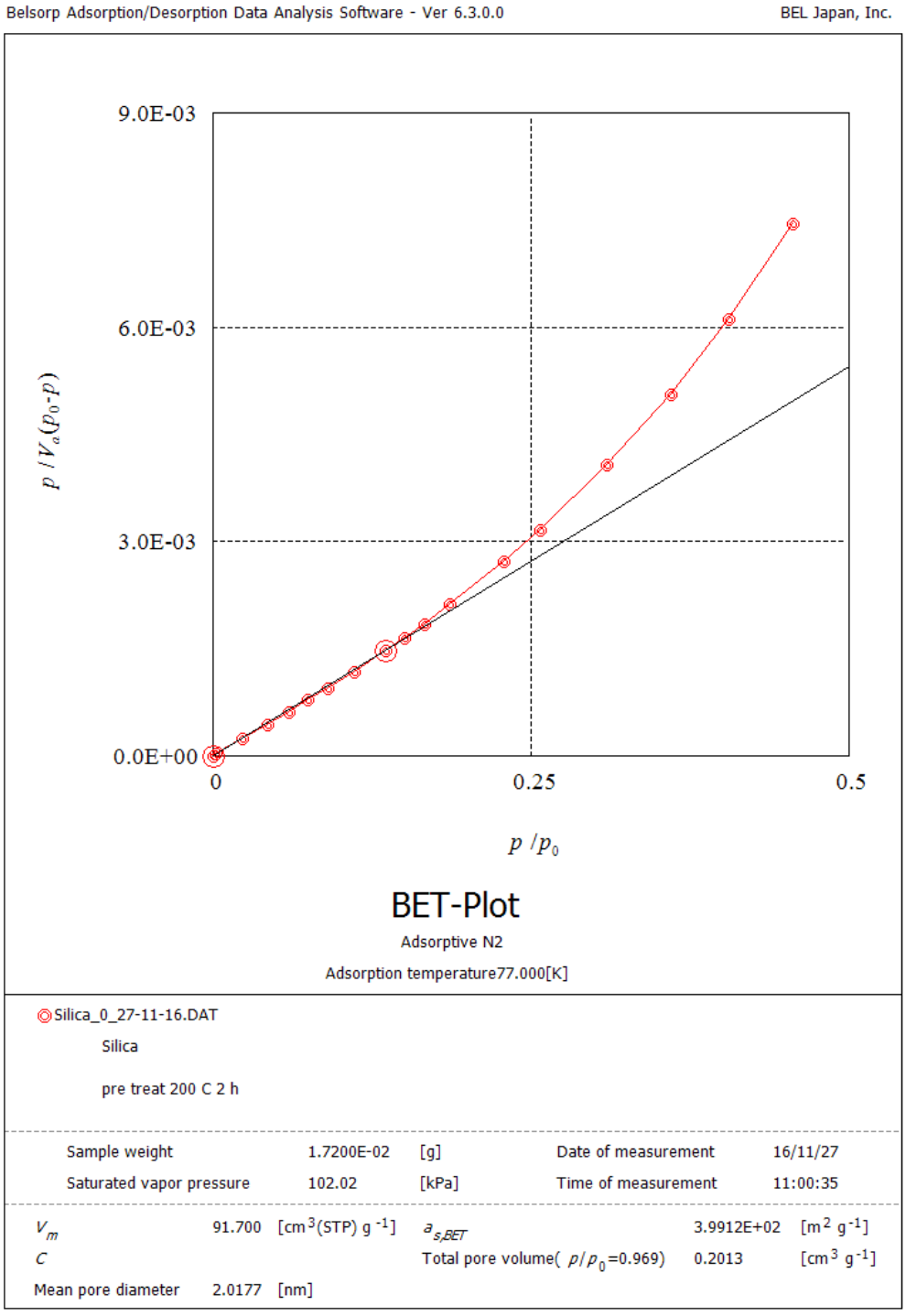

Figure A-2 BET-plot of Si_NF.

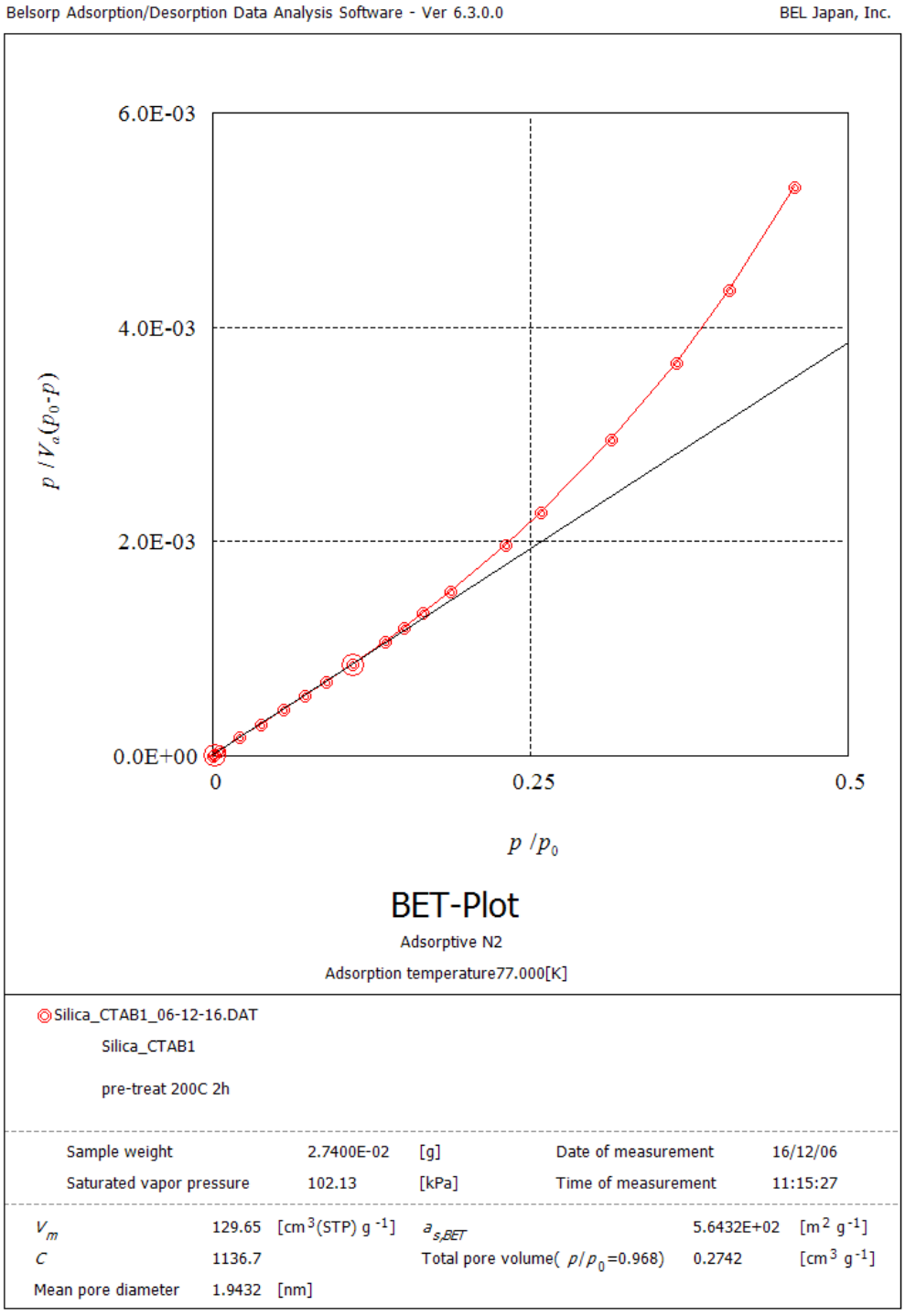

Figure A-3 BET-plot of Si_C-1.

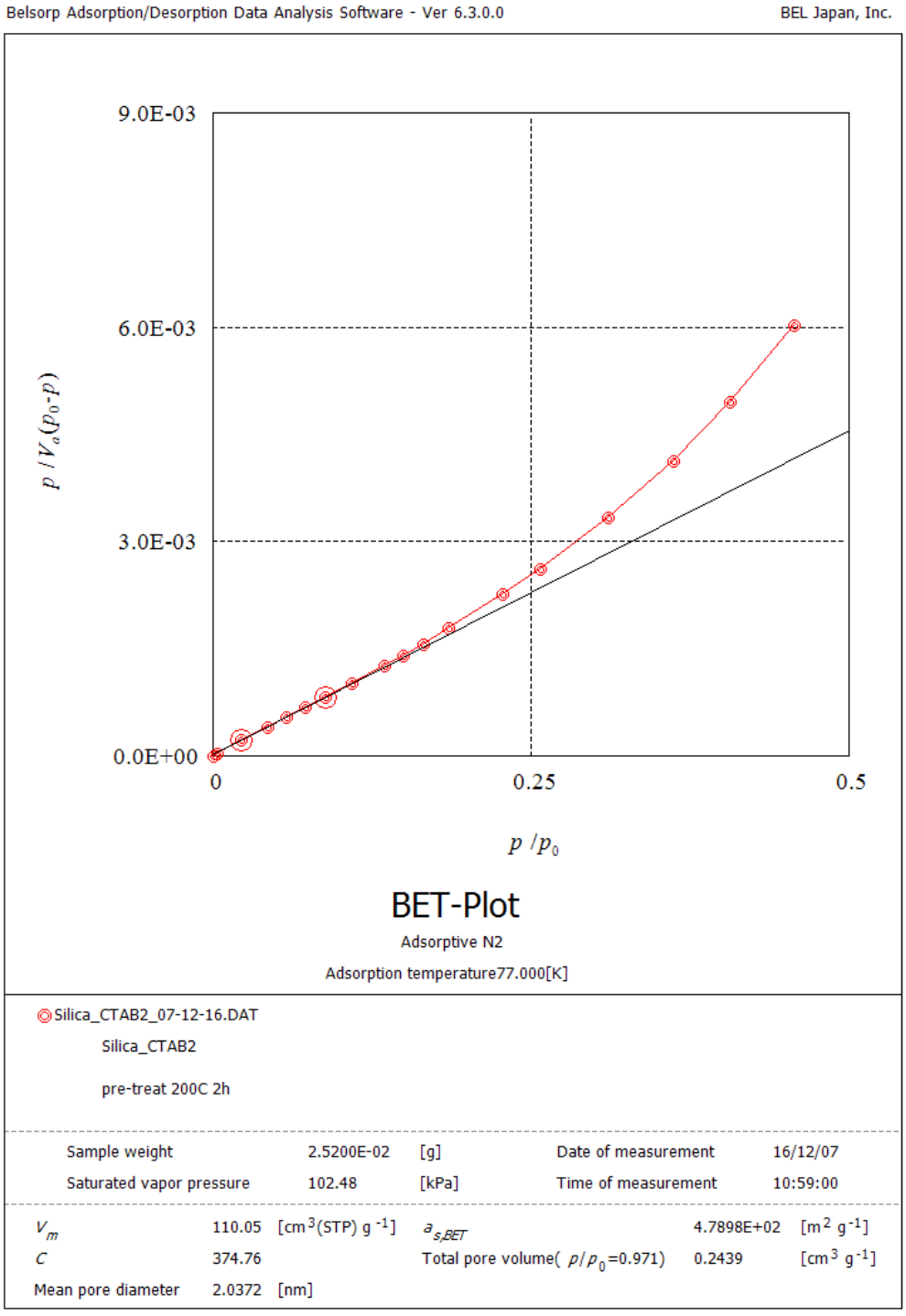

Figure A-4 BET-plot of Si_C-2.

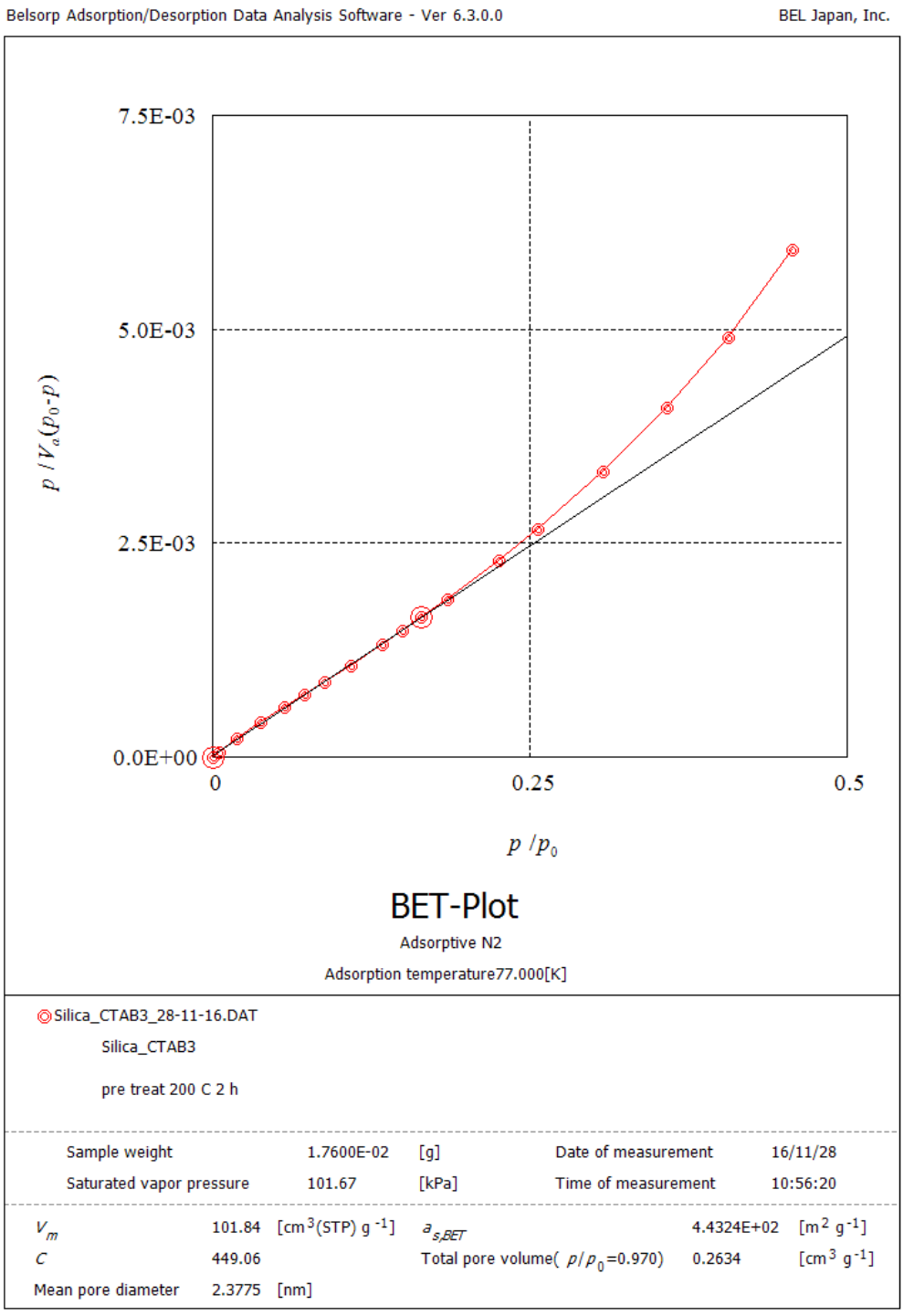

Figure A-5 BET-plot of Si_C-3.

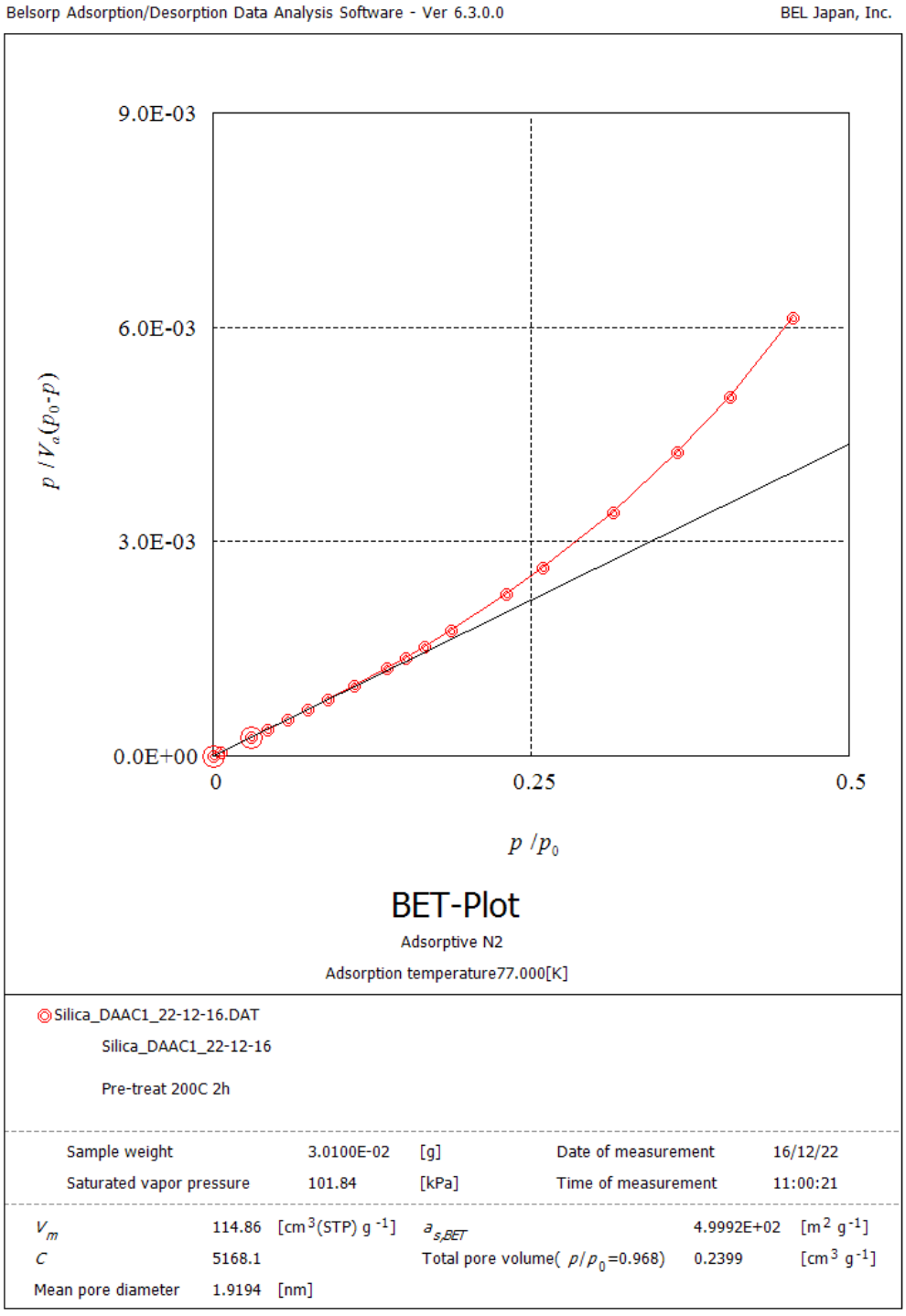

Figure A-6 BET-plot of Si_D-1.

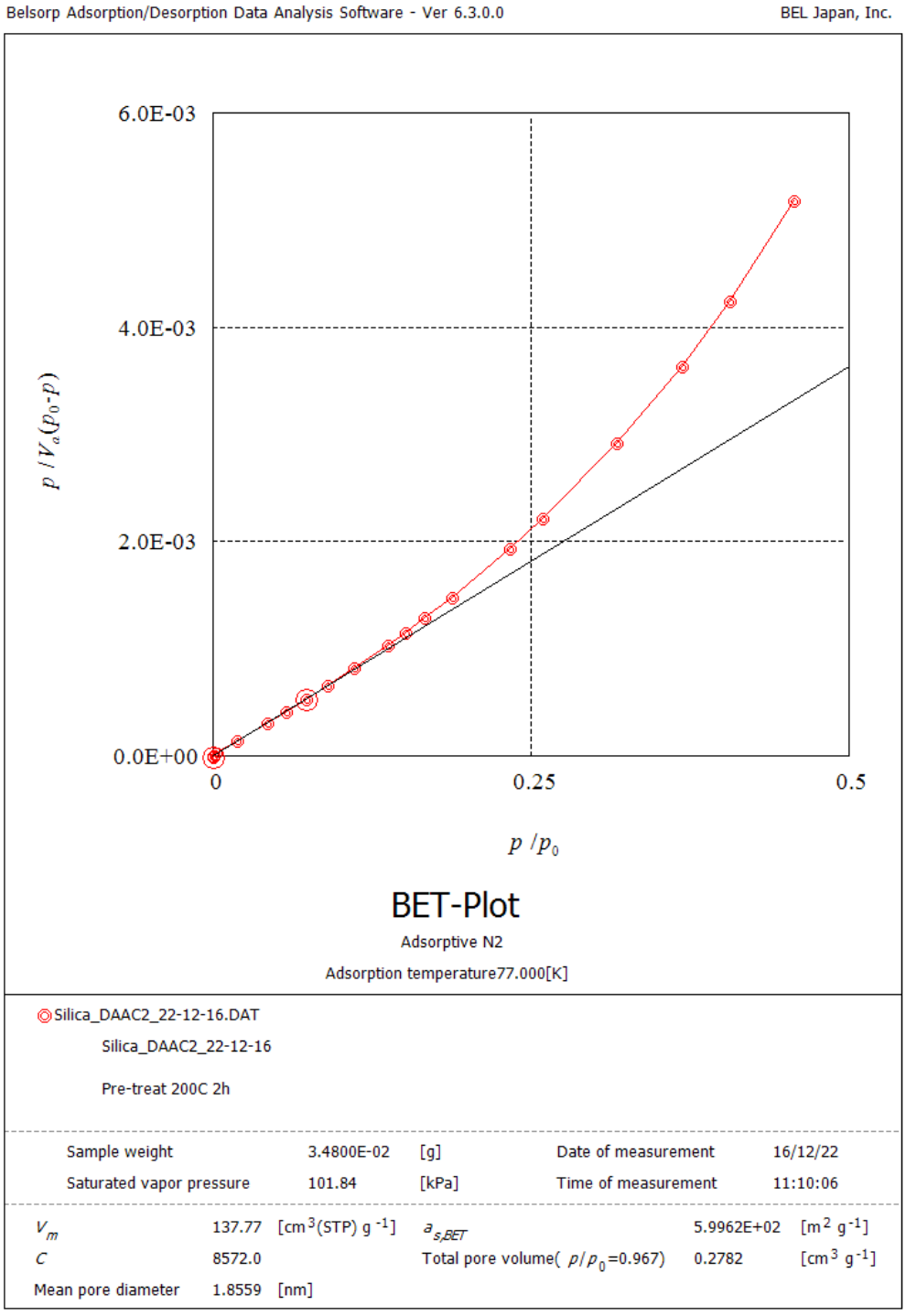

Figure A-7 BET-plot of Si_D-2.

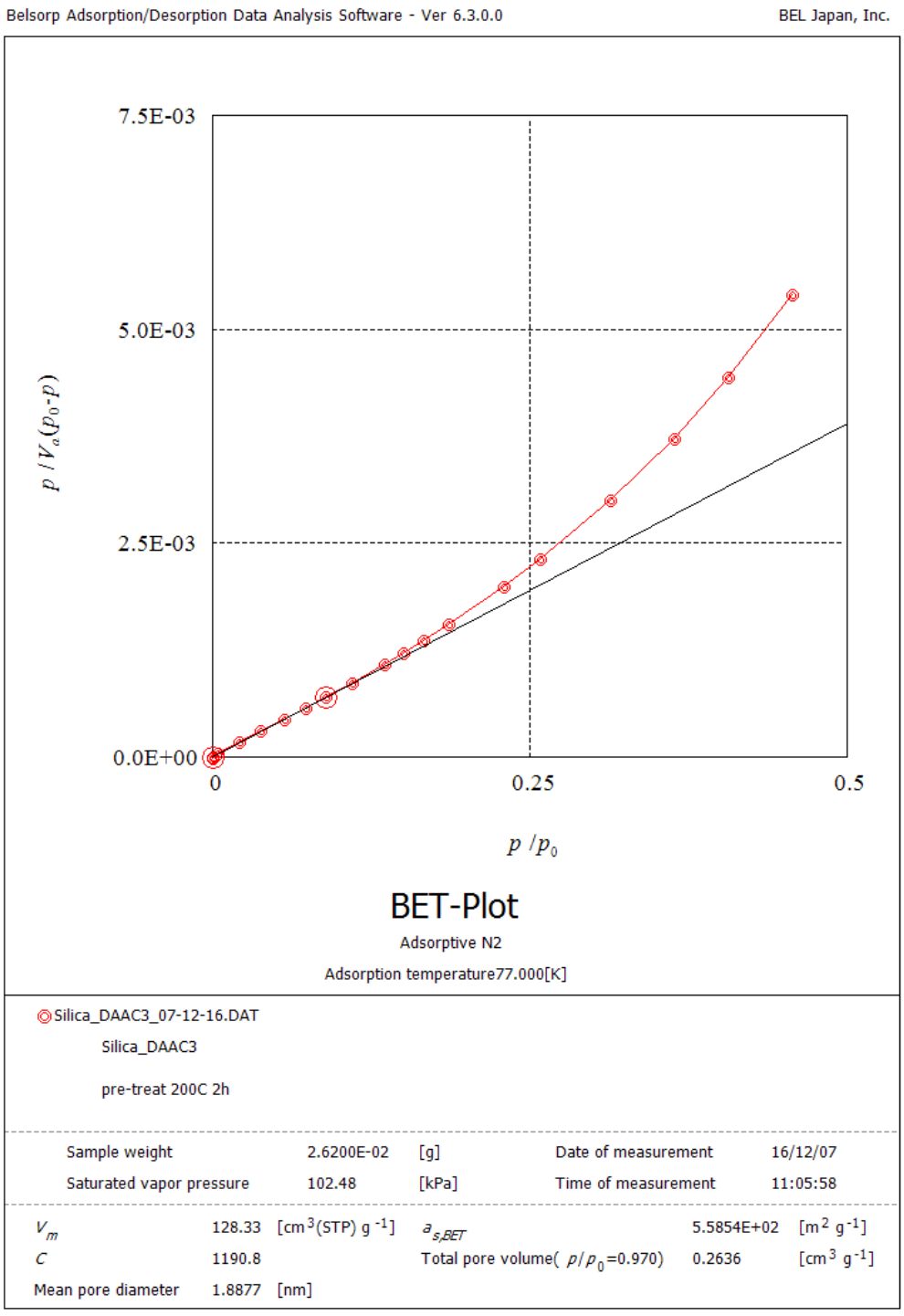

Figure A-8 BET-plot of Si_D-3.

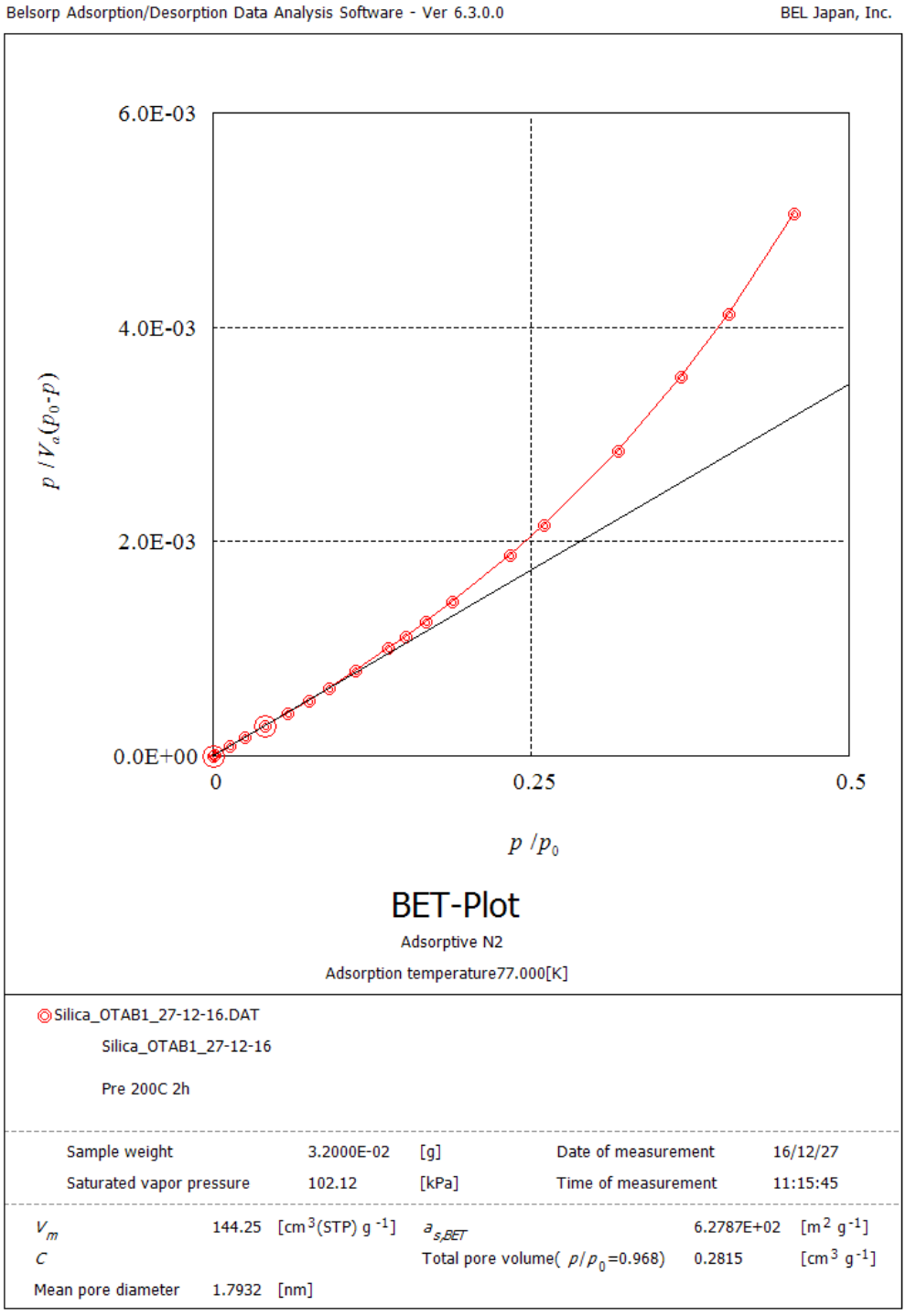

Figure A-9 BET-plot of Si_O-1.

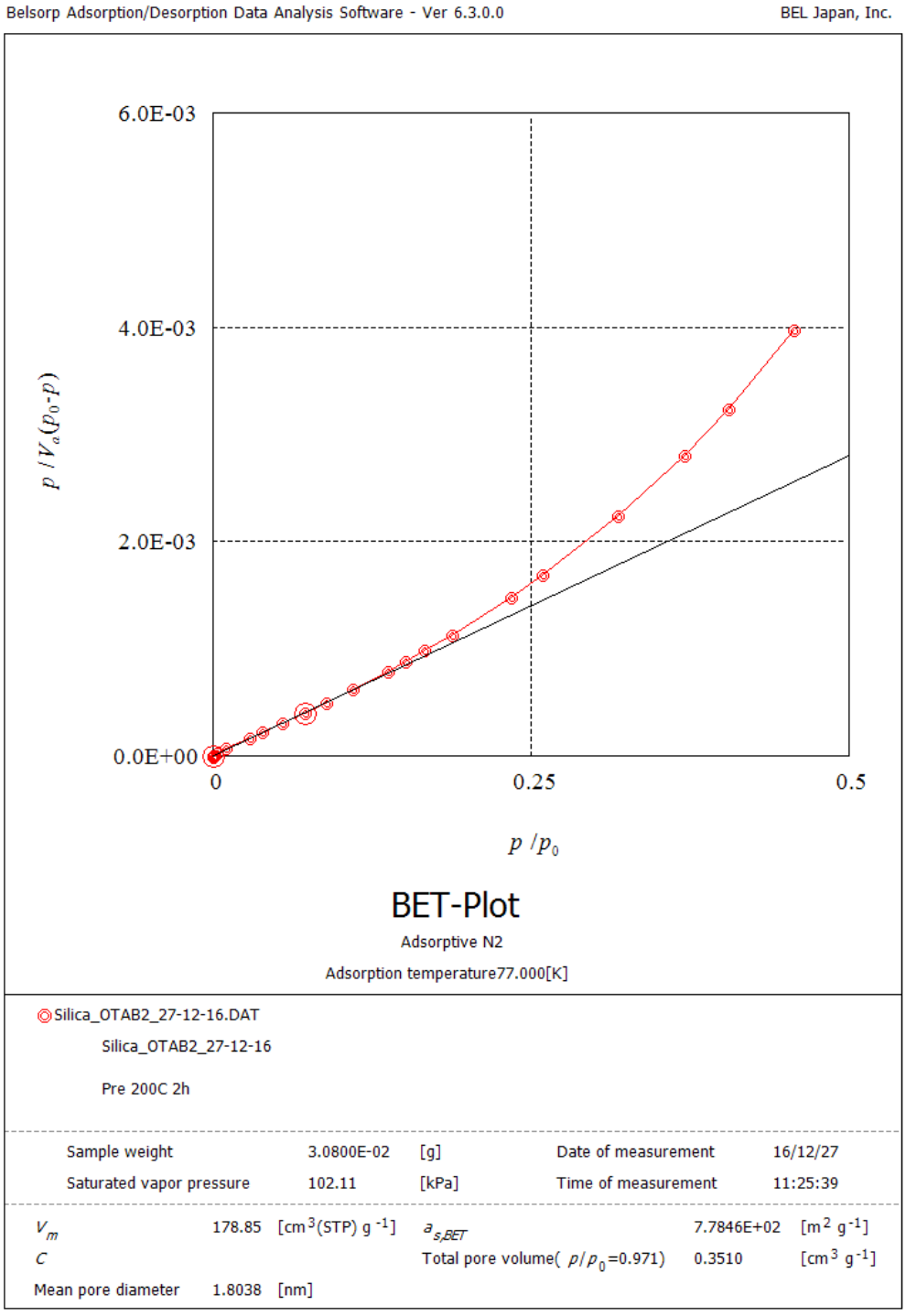

Figure A-10 BET-plot of Si_O-2.

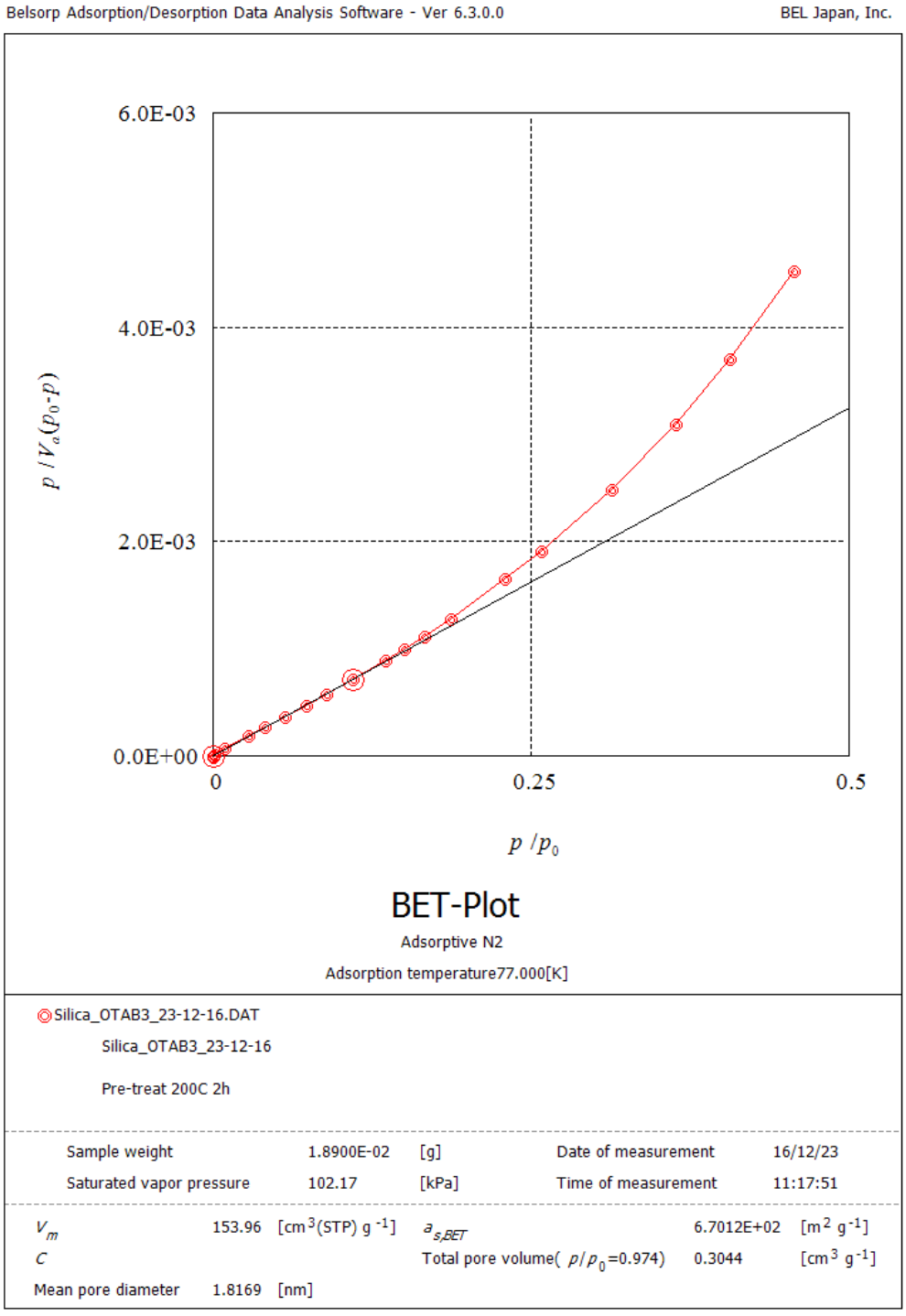

Figure A-11 BET-plot of Si_O-3.

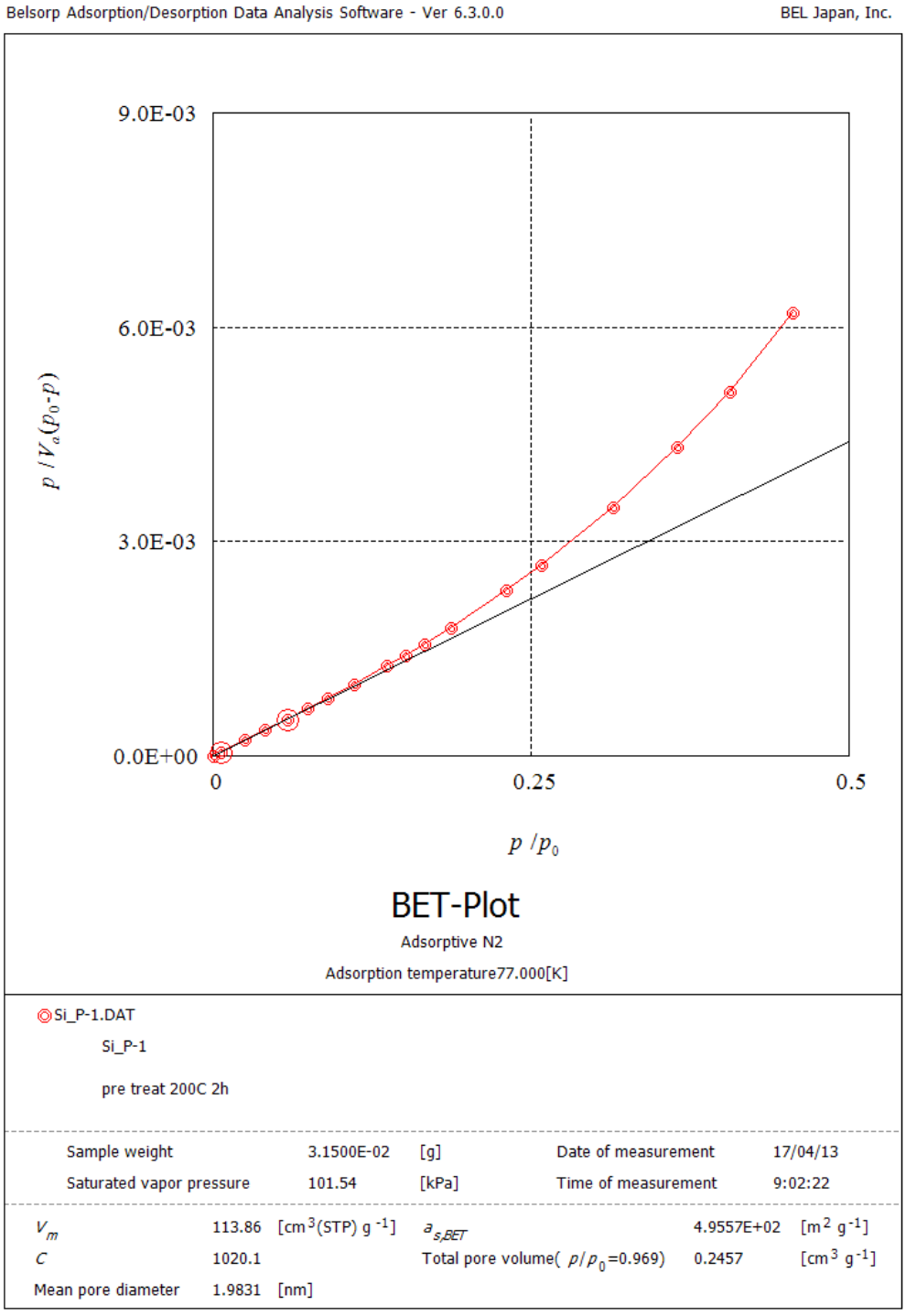

Figure A-12 BET-plot of Si_P-1.

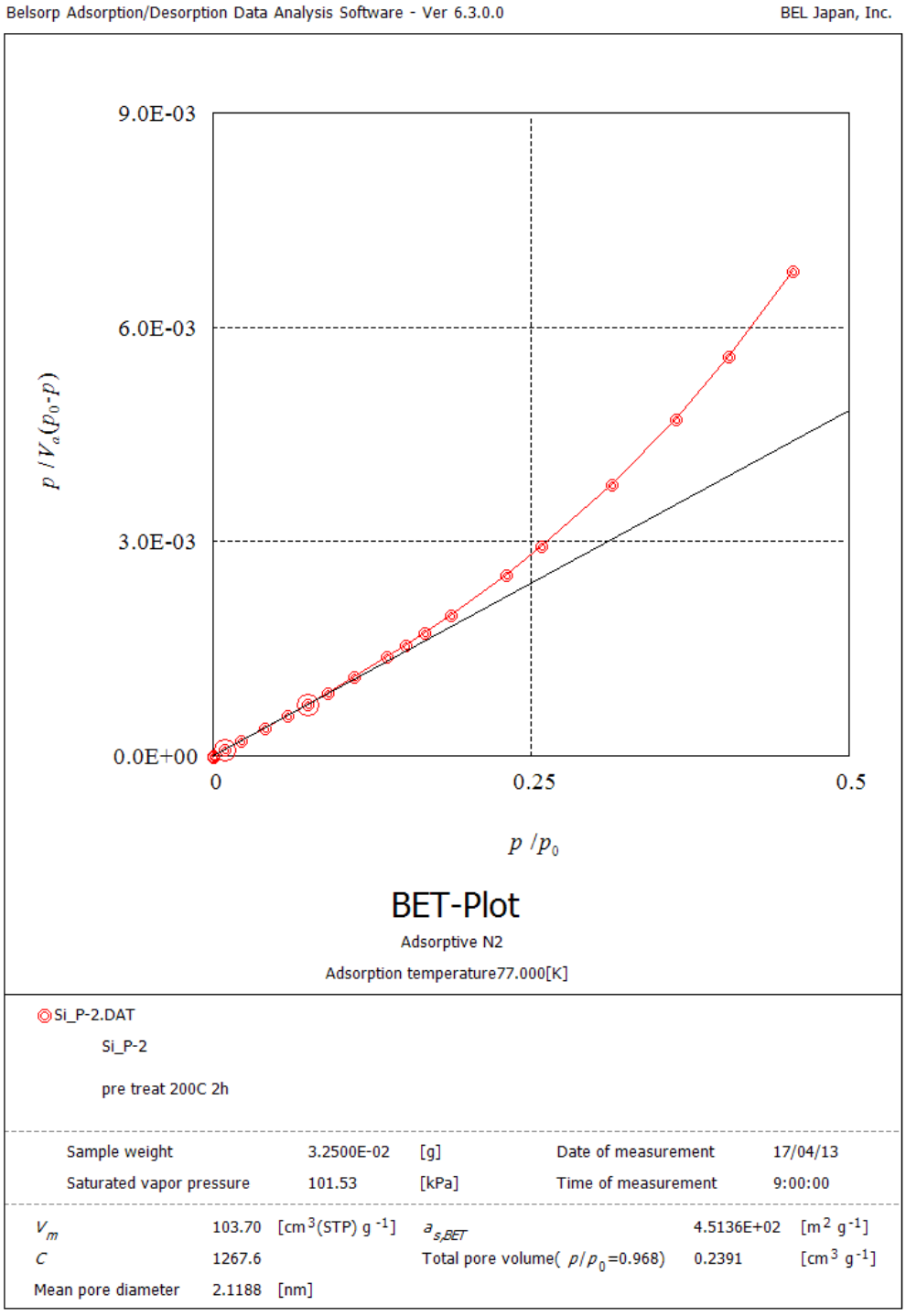

Figure A-13 BET-plot of Si_P-2.

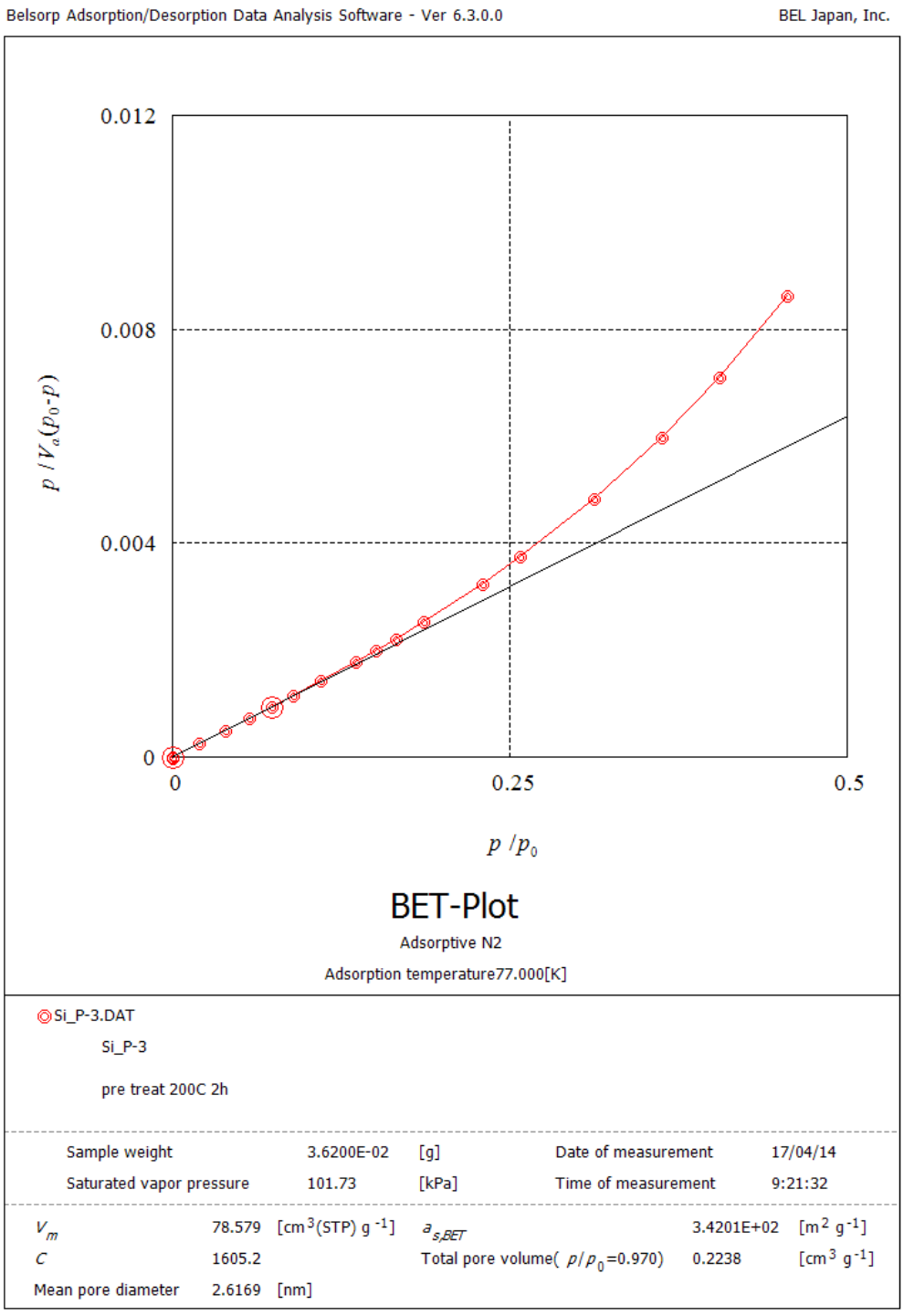

Figure A-14 BET-plot of Si_P-3.

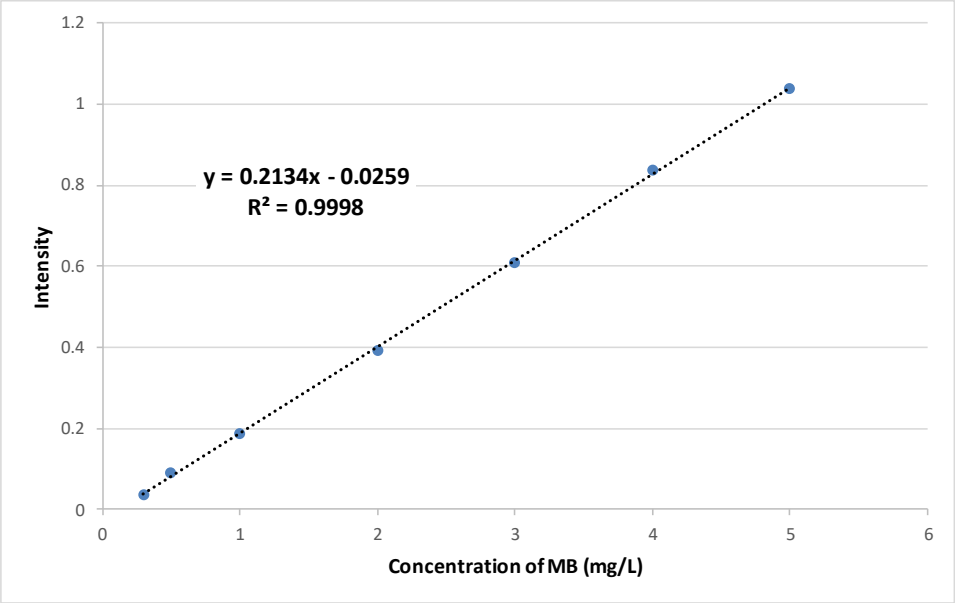

Figure A-15 Calibration curve of MB by UV-visible spectrophotometer.

Table A-1 Removal value of methylene blue when used fabricated silica nanofibers as adsorbent compared with silica gel. (n=3)

Surfactant	Silica nanofibers	Dye removal (%)	SD
-	Silica gel	74.4	0.8
-	Si_NF	79.5	0.4
CTAB	Si_C-1	93.0	0.5
	Si_C-2	88.2	1.3
	Si_C-3	85.9	0.9
DAAC	Si_D-1	93.8	1.1
	Si_D-2	96.3	0.4
	Si_D-3	94.8	0.9
OTAB	Si_O-1	96.3	0.3
	Si_O-2	97.5	0.2
	Si_O-3	93.7	1.5
PF	Si_P-1	95.2	1.8
	Si_P-2	88.0	1.3
	Si-_P-3	92.2	0.9

VITA

Miss Athchaya Suwansoontorn was born on June 27, 1992 in Bangkok, Thailand. She received her Bachelor's Degree of Science in Chemistry from Chulalongkorn University in 2014. After graduation, she continued with her graduate studies in the Analytical Chemistry Program, Faculty of Science, Chulalongkorn University. She finished her Master's degree of Science in 2017.

Poster presentation and proceeding

"The effect of cationic surfactant on porous structure in electrospun silica nanofibers" Athchaya Suwansoontorn, Puttaruksa Varanusupakul. Poster presentation and proceeding, Pure and Applied Chemistry International Conference 2017 (PACCON 2017), Centra Government Complex Hotel & Convention Center, Chaeng Watthana, Bangkok, Thailand, February 2-3, 2017.